Aalborg Universitet

Seismocardiography

Interpretation and Clinical Application

Sørensen, Kasper

Publication date:
2021

Document Version
Publisher's PDF, also known as Version of record

Link to publication from Aalborg University

SEISMOCARDIOGRAPHY: INTERPRETATION AND CLINICAL APPLICATION

BY
KASPER SØRENSEN

DISSERTATION SUBMITTED 2021

AALBORG UNIVERSITY
DENMARK

Seismocardiography: Interpretation and Clinical Application

Ph.D. Dissertation
Kasper Sørensen

CV

Kasper Sørensen

In 2015 Kasper Sørensen finished his Masters in Biomedical Engineering from Aalborg University and started working on his Ph.D. thereafter. In 2016 he received a Fulbright Scholarship and worked for four months as a guest researcher at the Biomedical Engineering Complex at the University of North Dakota, USA. Following this, Kasper completed a two-month research stay at Simon Fraser University in Vancouver, Canada. Kasper has participated in workshops and conferences within the field of cardiac mechanics as part of the Ph.D. and presented and discussed his work. Based on the research studies conducted throughout the Ph.D. peer-reviewed journal articles, conference proceedings, and abstracts have been published.

In the spring of 2017, Kasper started teaching at the Biomedical Engineering degree at Aalborg University in the course "Object Oriented Programming". In 2018 he co-founded the company VentriJect, a research-based company with roots in one of the studies that are part of this Ph.D.

Current position

2018-	Head of Software, VentriJect ApS
2018-	Part-time Lecturer, Aalborg University
2015-2020	Ph.D.-student at the Cardiotech Research Group, Aalborg University

Education

2015   M.Sc. in Biomedical Engineering and Informatics at Aalborg University

Selected Publications

2020

Sørensen K, Poulsen MK, Karbing DS, Søgaard P, Struijk JJ, Schmidt SE. A Clinical Method for Estimation of VO_2max Using Seismocardiography. In International Journal of Sports Medicine. 2020.

2019

Sørensen K, Struijk JJ, Jensen AS, Emerek KJG, Søgaard P, Schmidt SE. Changes of Seismocardiographic Intervals in Cardiac Resynchronization Therapy. In Annual Computing in Cardiology Conference, CinC. 2019.

Dehkordi P, Khosrow-Khavar F, Di Rienzo M, Inan OT, Schmidt SE, Blaber A, **Sørensen K**, et al. Comparison of Different Methods for Estimating Cardiac Timings: A Comprehensive Multimodal Echocardiography Investigation. In Frontiers in Physiology. 2019 aug 22;10. 1057.

Sørensen K, Poulsen MK, Karbing DS, Søgaard P, Struijk JJ, Schmidt SE. Correlation Between Valve Event Amplitudes in the Seismocardiogram and VO2-max. 2019. Abstract from Engineering in Medicine and Biology 2019, Berlin, Germany.

Munck K, Pedersen MW, Udesen NLK, Omar M, **Sørensen K**, Struijk JJ et al. Variation of the Seismocardiogram Depending on Measurement Position. In Annual Computing in Cardiology Conference, CinC. 2019

Munck K, **Sørensen K**, Struijk JJ, Schmidt SE. Visualization of the Multichannel Seismocardiogram. In Annual Computing in Cardiology Conference, CinC. 2019

2018

Sørensen K, Schmidt SE, Jensen AS, Søgaard P, Struijk JJ. Definition of Fiducial Points in the Normal Seismocardiogram. In Scientific Reports. 2018 okt 18;8(1). 15455.

Ulrich C, Jensen M, Hansen R, Tavakolian K, Khosrow-Khavar F, Blaber A, **Sørensen K**, Schmidt SE. Determining the Respiratory State From a Seismocardiographic Signal: A Machine Learning Approach. In Annual Computing in Cardiology Conference. 2018;45.

Munck K, Schmidt SE, **Sørensen K**, Struijk JJ. Multichannel Seismocardiography: A Novel Method for Investigating the Seismocardiogram. 2018. In Annual Computing in Cardiology Conference, 2018, Maastricht, Holland.

2017

Sørensen K, Verma AK, Blaber A, Zanetti J, Schmidt S, Struijk JJ, et al. Challenges in using seismocardiography for blood pressure monitoring. In Annual Computing in Cardiology Conference, 2017, Rennes, France.

Thomsen LP, Aliuskeviciene A, **Sørensen K**, Nørgaard AC, Sørensen PL, Mark EB, et al. Non-invasive estimation of respiratory depression profiles during robot-assisted laparoscopic surgery using a model-based approach. In Badnjevic A, red., CMBEBIH 2017: Proceedings of the International Conference on Medical and Biological Engineering 2017. Springer. 2017. s. 223-231. (IFMBE Proceedings; Nr. 62).

Sørensen K, Jensen AS, Hansen J, Søgaard P, Struijk JJ, Schmidt S. Seismocardiographic correlations to age, gender and BMI. 2017. Abstract from 39th Annual International Conference of the IEEE Engineering in Medicine and Biology Society, EMBS, EMBC 2017, Jeju Island, South Korae.

2016

Sørensen K, Schmidt SE, Sørensen PL, Korsager AS, Melgaard J, Søgaard P o.a. Automatic segmentation of mitral leaflet movement in Doppler Tissue M-Mode ultrasound. In Annual Computing in Cardiology Conference, 2016, Vancouver, Canada.

Munck K, Hansen BD, Jacobsen N, Pilgaard LP, Schmidt SE, **Sørensen K**, et al. Body surface mapping of the mechanical cardiac activity. In Annual Computing in Cardiology Conference, 2016, Vancouver, Canada.

Melgaard J, Graff C, Sørensen PL, **Sørensen K**, Schmidt S, Struijk JJ. Effect of sample rate on saECG spectrum. In Annual Computing in Cardiology Conference, 2016, Vancouver, Canada.

Struijk JJ, Munck K, Hansen BD, Jacobsen N, Pilgaard LP, **Sørensen K**, et al. Heart-valve sounds obtained with a laser Doppler vibrometer. In Annual Computing in Cardiology Conference, 2016, Vancouver, Canada.

Schmidt SE, Emerek KJG, Jensen AS, Graff C, Melgaard J, Søgaard P, **Sørensen K** and Struijk JJ. Temporal alignment of asynchronously sampled biomedical signals. In Annual Computing in Cardiology Conference, 2016, Vancouver, Canada.

Sørensen PL, **Sørensen K**, Melgaard J, Struijk J, Hansen SM, Kanters JK, et al. Vectorcardiographic quantification of early repolarization. In Annual Computing in Cardiology Conference, 2016, Vancouver, Canada.

Patents

2019

Schmidt SE, **Sørensen K**, Søgaard p and Struijk JJ. Cardiovascular and cardiorespiratory fitness determination. WO2017216375A1

Based on the studies carried out in the thesis, the following three papers were produced. These papers are considered the thesis papers.

Paper I   **Sørensen K**, Schmidt SE, Jensen AS, Søgaard P, Struijk JJ.
Definition of Fiducial Points in the Normal Seismocardiogram.
Published in: Scientific Reports. 2018 okt 18; 8(1). 15455.

Paper II   **Sørensen K**, Søgaard P, Emerek K, Jensen AS, Struijk JJ, Schmidt SE.
Seismocardiography as a Tool for Assessment of Bi-Ventricular Pacing.
In review at: Frontiers in Physiology - Cardiac Vibration Signals: Old Techniques, New Tricks and Applications. November 2020.

Paper III   **Sørensen K**, Poulsen MK, Karbing DS, Søgaard P, Struijk JJ, Schmidt SE.
A Clinical Method for Estimation of VO_2max using Seismocardiography.
Published in: International Journal of Sports Medicine. Vol 41. Issue 10. September 2020.

Abbreviations

AC	Aortic Valve Closure
AO	Aortic Valve Opening
CCT	Cardiac Computer Tomography
CMRI	Cardiac Magnetic Resonance Imaging
CRT	Cardiac Resynchronization Therapy
CTI	Cardiac Timing Interval
CVD	Cardiovascular Disease
ECG	Electrocardiography
EDV	End Diastolic Volume
ESV	End Systolic Volume
g	Gravitational Constant ($\sim 9.82 \mathrm{m} \cdot \mathrm{s}^{-2}$)
HR	Heart Rate
IC4	Inter Costal Space 4
LV	Left Ventricle
MC	Mitral Valve Closure
MEMS	Micro Electro-Mechanical System
MO	Mitral Valve Opening
ms	Milliseconds
S1	First heart sound
S2	Second heart sound
SCG	Seismocardiography
SEE	Standard Error of Estimate
SSE	Sum of Squared Error
SV	Stroke Volume
PCG	Phonocardiography
PPG	Pulse Plethysmography
RV	Right Ventricle
VO_2max	Maximal Oxygen Consumption

Abstract

Cardiovascular disease (CVD) is the leading cause of death and in Europe alone it is accountable for 3.9 million deaths every year. Even though the number of deaths is declining, morbidity is not, leading to the low quality of life for the people affected. A wide variety of diagnostic tools for CVD exist, each within their field of application. Electrocardiography (ECG) is used to assess and analyze the electrical activation of the heart, whereas echocardiography (echo) is used to produce ultrasound images of the heart as it contracts and relaxes, giving insight into the mechanical activation of the heart muscle. In this project, the method of recording cardiac vibrations non-invasively on the sternum, called seismocardiography (SCG), is investigated.

The thesis is composed of three studies. The first study investigates the origin of the signal with respect to the underlying physiology determined with echo from 45 healthy subjects. This study contributes to the overall understanding of the correlation between deflections in the signal and physiologic events in the cardiac cycle. The second study focuses on the manifestation of the signal in patients with cardiac resynchronization therapy (CRT) pacemakers. Further, the study explores the possibility of using SCG for optimization of the pacing delay setting of the pacemaker. The third study evolves around the correlation between features in the SCG signal and cardiorespiratory fitness.

Study I demonstrate the physiologic connection between the SCG and events found in echo. Eight fiducial points in the SCG have short temporal distance and high correlation to eight physiologic events found in echo. Study II shows how the mechanical dyssynchrony manifests in the SCG signal and how cardiac time intervals that are derived from the SCG changes with different pacing settings. In Study III, gold standard VO_2max was measured, and a model for non-exercise VO_2max estimation with the SCG signal was developed.

The SCG carries complex and valuable information about cardiac mechanics. This thesis identifies some of the underlying physiological origins of the signal and demonstrates two clinical use cases for the method: Bi-ventricular pacemaker optimization and estimation of VO_2max.

Resumé

Kardiovaskulær sygdom er den ledende årsag til død og er i Europa alene skyld i 3.9 millioner dødsfald hvert år. Til trods for at antallet af dødsfald er faldende, er sygeligheden ikke, hvilket resulterer i lav livskvalitet for patienter der er påvirkede af sygdommen. Der findes en række kliniske diagnostiske værktøjer til undersøgelse af kardiovaskulær sygdom, der hver har sine anvendelsesområder. Elektrokardiogram (EKG) bruges til at måle den elektriske aktivitet i hjertet, mens ekkokardiografi (ekko) bruges til at producere ultralydsbilleder af hjertet mens det trækker sig sammen og slapper af. I dette projekt undersøges en metode til optagelse af vibrationerne der opstår som følge af hjertets sammentrækning, kaldet seismokardiografi (SKG).

Denne afhandling er opbygget af tre studier. Det første studie undersøger signalets fysiologiske oprindelse ved brug af ekko fra 45 raske forsøgspersoner. Dette studie bidrager til den grundlæggende forståelse af signalet og dets relation til de forskellige stadier i hjertets cyklus. Det andet studie undersøger hvordan signalet manifesteres hos patienter med kardial resynkroniseringsterapi (KRT) pacemaker. Studiet udforsker endvidere hvordan SKG kan anvendes til at optimere indstillingerne for pacemakeren. Det tredje studie omhandler sammenhængen mellem SKG signalet og kardiorespiratorisk fitness.

Studie I demonstrer den fysiologiske forbindelse mellem SKG signalet og stadierne i hjertets sammentrækning. Otte reference punkter i SKGet har lav temporal distance og høj korrelation til fysiologiske markører i ekko. Studie II viser hvordan mekanisk dyssynkroni manifesteres i SKGet og hvordan tidsintervaller udregnet på baggrund af signalet ændres med forskellige pacing indstillinger. I studie III måles VO_2max med ergometer test og en model for estimering af VO_2max ved brug af SKG i hvile blev udviklet.

SKG signalet indeholder kompleks og værdifuld information omkring hjertets mekaniske sammentrækning. Denne afhandling identificerer noget af den underlæggende fysiologi samt demonstrerer to brugsscenarier for metoden: optimering af bi-ventrikulær pacemaker og estimering af VO_2max.

Acknowledgements

This Ph.D. thesis and the studies in it could not have been completed without the assistance from my supervisors, colleagues, my family, and my friends.

First I would like to thank my main supervisor professor Johannes Jan Struijk. Johannes has been a great inspiration throughout my Ph.D. and has always been extremely helpful when I was struggling with my papers. I could always count on Johannes to read a manuscript two hours before a deadline and give me feedback that would enhance the content of the paper. I would also like to thank my co-supervisor associate professor Samuel Emil Schmidt. Samuel has always kept me intrigued with our research, he has always shared his great ideas, and helped me tremendously with my data analysis and article writing. Samuels passion for "accessible technology" has been a huge inspiration to me. I am also very grateful that Samuel asked me to be a part of the "VentriJect-team" and made it possible for me to stay at Aalborg University.

A big thanks to all my colleagues, especially from the Cardio Technology Research Group at Aalborg University, Claus Graff, Jacob Melgaard, and John Hansen. To my collaborators at Aalborg University Hospital, Peter Søgaard, and Kasper Emerek thank you. Mathias Krogh Poulsen and Dan Stieper Karbing from AAU, thank you for your valuable feedback within the field of respiratory fitness.

I would also like to thank Dr. Kouhyar Tavakolian for having me as a guest researcher at the University of North Dakota as well as all the great people I met in Grand Forks and Vancouver: Vera-Ellen Lucci, Malcom Tremblay, Ajay K. Verma, and Charles Michael Schneider. Likewise, I am very thankful that I had the opportunity to meet and work with one of the early pioneers within seismocardiography before his passings, John Zanetti.

I also thank the foundations that have supported me with funding for research, travels, and conferences: Knud Højgaards Fonden, Kong Christian d. 10. Fond, Augustinus Fonden, and Fulbright Denmark.

To Jonna, Jens, Sinna, Karen and Poul

Preface

This Ph.D. thesis has been submitted to the Doctoral School in Medicine, Biomedical Science and Technology at Aalborg University. The research was conducted at Aalborg University, Denmark from August 2015 to August 2020. The Ph.D. study was financially supported by the Independent Research Council (Det Frie Forskningsråd). The study was supervised by professor Johannes J. Struijk and associate professor Samuel E. Schmidt at Aalborg University.

The thesis is based on three studies within the field of cardiac microvibrations recorded with an accelerometer, a method called Seismocardiography. The reader is advised to have some physiologic and anatomical knowledge about the heart. The thesis consists of an introduction and background chapters, followed by a chapter describing the method used throughout all three studies. Methods specific for each of the studies will be presented in the chapter "Summary of Thesis Studies". Summary of the main findings, discussion along with future perspectives and the conclusion of the thesis follows.

<div align="right">
Kasper Sørensen

Aalborg University, July 6, 2021
</div>

Contents

Introduction

Cardiovascular disease (CVD) is responsible for 3.9 million deaths in Europe every year and the number one cause of death [1]. CVD is also the leading cause of morbidity in Europe and even though the number of deaths from CVD is declining, this is not the case for morbidity [1]. The morbidity means lower life quality for the people affected, with small everyday tasks like putting on clothes, cleaning the house, and engaging in hobbies becoming hard to overcome.

While the prevalence of factors such as smoking, alcohol consumption and mean blood cholesterol are declining, some more than others, the prevalence of overweight, obesity, and diabetes has increased in the recent decade [1, 2]. This has raised concern about the sustainability of the reduction in mortality [1, 3]. Improvements in health care treatment, an increase in the general population size, and especially older people, contribute to the increase in morbidity [2]. In the European Union (EU) almost 49 million people live with a CVD (numbers from 2015) which is estimated to cost the EU €210 billion each year [1]. This economic burden is not only observed in the EU but also in the United States and worldwide [2, 4]. In 2010 16.7 million deaths worldwide were attributed to CVD and the projection for 2030 is 23.3 million deaths [2].

Diagnosis of CVD ranges from blood pressure measurements over echocardiography, phonocardiography, cardiac X-ray to cardiac magnetic resonance imaging, single-photon emission computed tomography, and electrocardiography to name some. All these modalities contribute to separate areas of determining the diagnosis. This thesis aims to explore the modality seismocardiography to investigate both the physiologic origin of the signal and the potential clinical use cases, as a relatively simple to use, non-invasive cardiac monitoring device.

Chapter 1. Introduction

Background

The following chapter will go through the history of the seismocardiogram, the origin, and evolvement of the method with reference to noteworthy studies, and some of the latest use cases and applications for the method. This chapter should bring insight into how the technology came to be and the current state of the art with alternative methods to seismocardiography. First, a brief introduction to the normal heart and some of the current clinically available tools for assessing the mechanical condition of the heart.

2.1   The Electrical Conduction Pathway and Mechanical Contraction of the Heart

The electrical conduction pathway in the healthy heart ensures a synchronized and repetitive automatic contraction of the muscle fibers of the heart [5]. The conduction pathway includes: the sinoatrial (SA) node located in the posterior wall of the right atrium and the atrioventricular (AV) node located right atrium close to the coronary sinus, see Figure 2.1 [5]. These two nodes are connected via internodal pathways. From the AV node, the bundle of His travels through the superior part of the septal wall, before dividing into the left and right bundle branches. From the two bundle branches the conduction pathway is separated into the purkinje fibers that encase the two ventricles [5, 6].

The SA and AV nodes are made up of pacemaker cells. As the membranes of these cells cannot maintain a stable resting potential, after repolarization the membrane potential will drift towards a threshold and upon reaching the threshold, the cells depolarize spontaneously [5, 6]. With no hormonal or neural regulation action potentials are generated about 80-100 times a minute in the SA node, compared to 40-60 times a minute in the AV node [5]. Because depolarization is more frequent in the SA node than the AV node, the SA node initiates the atrial contraction and controls the heart rate. The electrical impulse spreads from the SA node, through the internodal pathways and the contractile cells to the AV node, causing the right and left atrium to contract
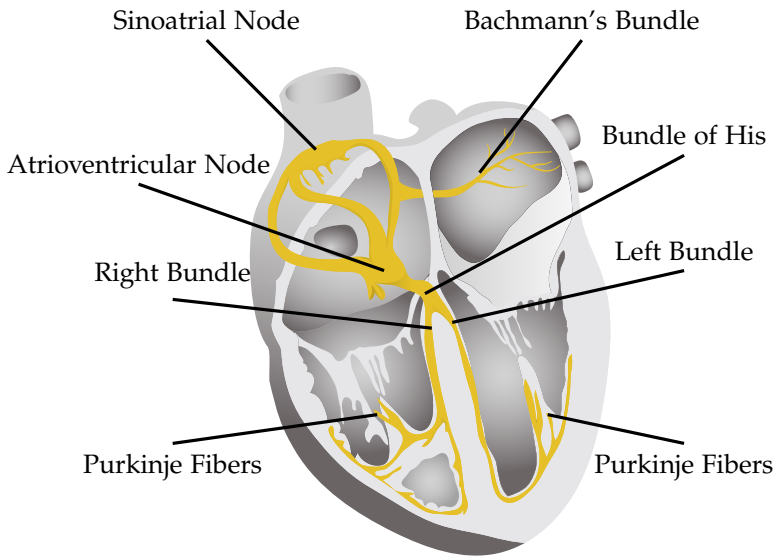
Fig. 2.1: The electrical conduction system of the heart. Reprinted with permissions (Adobe Standard License).

[5, 6]. The slower activation and conduction of the AV node introduces a natural delay in the conduction of the electrical impulse and thus a delay between atrial and ventricular contraction. From the AV node, the electrical activity spreads through the bundle of His, the bundle branches and at last the purkinje fibers. Compared to the rest of the conduction system, the cells in the Purkinje fibers are larger in diameter and thus conduct the action potentials faster than other cells [5].

See Figure 2.2 for anatomical reference of the heart and Figure 2.3 for reference to the normal cardiac cycle. The conduction system serves to spread the action potential throughout the myocardium to facilitate a synchronous mechanical contraction of the heart. By convention, this starts just before the atrial contraction. At this point the ventricles are relaxed after the previous contraction, see Figure 2.3 (1) Diastole, and blood is filling the left and right atrium. Due to the relaxation in the ventricles, the pressure gradient between the ventricles and the aorta and pulmonary trunk respectively have caused the aortic and pulmonary valves to close. At this point the tricuspid and mitral valves are also closed; this is the iso-volumetric relaxation period (IVRT). When the pressure in the ventricles falls below that of the atria, the tricuspid and mitral valves open, and blood starts to fill the ventricles, see Figure 2.3 (2) Diastole [5, 6]. This initial filling caused by the atrioventricular pressure
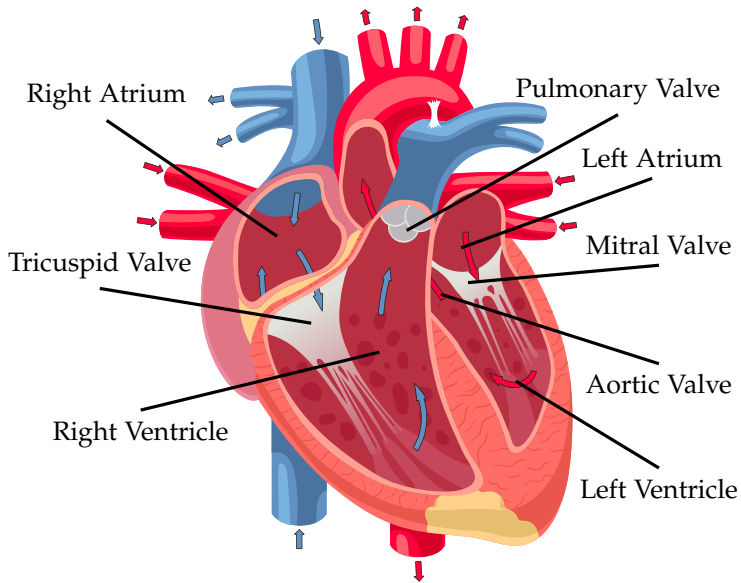
Fig. 2.2: Anatomy of the normal human heart. Note that the aortic valve is located under the area of the pulmonary valve in this illustration. Reprinted with permissions (Adobe Standard License).

gradient is called the rapid filling phase. As blood fills the ventricles the pressure gradient diminishes and the filling of the ventricle stops briefly, before the atrial contraction forces additional blood into the ventricles, see Figure 2.3 (3) Atrial Systole [6]. In the ventricular systole, blood is forced towards the tricuspid and mitral valves, causing them to close, see Figure 2.3 (4) Ventricular Systole. With the valves closed, pressure in the ventricles builds up, as the volume of the blood cannot change; this is the iso-volumetric contraction period (IVCT). The contraction of the heart causes the shape of the heart to become more spherical as the pressure builds up. When the pressure in the ventricles exceeds the pressure in the pulmonary trunk and the aorta, the pulmonary and aortic valves open and blood flow into the pulmonary and systemic system, see Figure 2.3 (5) Ventricular Systole, [5, 6]. With the emptying of the ventricles, the shape of the heart "flattens" to a more cone-like shape. Following the contraction, the ventricles start to relax and the heart cycle is completed.
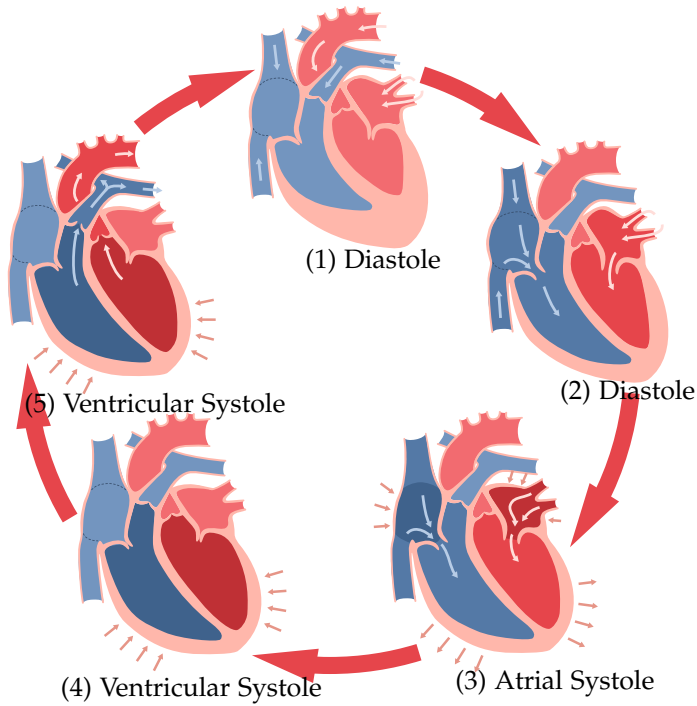
Fig. 2.3: Five stages of the normal cardiac cycle. White arrows indicate blood flow and red arrows indicate muscle contraction and relaxation. (1) Diastole: blood flow into the atria. (2) Diastole: passive blood flow into the ventricles. (3) Atrial systole. (4) Ventricular systole, pressure builds in the ventricles. (5) Ventricular systole, blood is forced into the pulmonary trunk and aorta. Reprinted with permissions (Adobe Standard License).

2.2 Current Clinical Diagnostic Methods

This section aims to provide an insight into some of the cardiac modalities currently used in the clinic. The selection of technologies includes some of the most common and non-invasive diagnostic methods that have also been used in this thesis. Going into detail with each of these technologies is outside of the scope of this thesis; this section serves to give an overview of current technologies and some of their clinical applications and limitations.

2.2.1 Phonocardiography

In 1894 Einthoven and Geluk made the first true electrical recording of the heart sounds [7]. The sounds primarily arise from the closing but also to some

degree the opening of the heart valves. The first and second heart sound (named S1 and S2) originates from the closure of the atrioventricular valves and closure of the semilunar valves, respectively [6, p. 259-288]. This gives rise to the well known "lubb-dubb" sound pattern. The heart sounds facilitate the assessment of cardiac conditions with respect to the mechanical contraction of the heart [6, p. 259-288]. Murmurs, delays between the sounds, splitting of the sounds, and missing sounds are used to diagnose different cardiac conditions. For instance, mitral valve regurgitation can be heard as a murmur caused by the turbulent flow of blood through the mitral valve. In the clinic, the PCG is not commonly recorded and analyzed, but the auscultations from the heart are obtained with a stethoscope and interpreted by the clinicians on site.

2.2.2 Electrocardiography

The electrocardiogram (ECG) is likely the most well known cardiac modality [8]. Einthoven published his first paper about the device for recording the ECG (the string galvanometer) in 1901 and the first application of use in 1903 [8, 9]. In contrast to the phonocardiogram, the ECG presents the electrical activity of the heart. Different configurations of the ECG exist, with the common 12-lead ECG obtained using electrodes placed on the chest, wrist, and ankles of the patient [6, p. 295-300]. The electrodes record the electrical field originating from the heart, as the muscle contracts. Using multiple electrodes it is possible to assess the electrical contraction force from different angles [6, p. 295-300]. The electrical activation is naturally related to the contraction of the heart muscle, thus the ECG can be used to diagnose a wide variety of cardiac conditions such as the electrical conduction pathways of the heart, hemodynamics, and drug-induced abnormalities [6, 8].

2.2.3 Echocardiography

Echocardiography (often referred to as "echo") utilizes high frequency sound waves, ultrasound, to produce an image of the heart [6, p. 351-458]. The technology dates back to 1954 [10]. A probe connected to the ultrasound machine serves to send and receive the sounds. Scanning multiple physiologic planes and angling the probe in different orientations, helps the clinician to obtain an insight into the heart of the patient [6, p. 351-458]. With echocardiography, it is possible to obtain information about the mechanical contractions of the heart with the opening and closing of the valves [6, p. 351-458]. Further, the use of echo doppler allows sampling of the blood flow in the ventricles, the aortic arch, and more [11]. Thus, the modality is very versatile, but it requires specially trained clinicians to perform echocardiographic recordings and interpret the images.

2.2.4 Challenges with Current Clinical Diagnostic Methods

The current cardiac modalities used in the clinic provide physicians with insights into the mechanical and electrical conditions of the heart. This of cause raises the question if there is a need for a new cardiac modality. The modalities presented in the sections above all have different advantages with assisting the clinicians in determining the condition of the heart in different ways. But they also present some limitations.

The PCG signal is good for indicating when the valves in the heart close, as this gives rise to the sounds, and a skilled clinician can determine cardiac conditions by listening to the auscultations. However, the opening of the valves can be difficult to accurately locate, making cardiac timing intervals impossible to calculate. Defining exactly when a valve closes does also seem to be ambiguous [12]. The ECG requires electrodes to be attached to the patient and in the case of a 12-lead, this amounts to ten electrodes. If these are not placed correctly, the ECG can manifest incorrectly and in the worst case potentially lead to wrong diagnosis [13]. Further, the ECG only represents the electrical forces of the heart. In some cases the ECG does not give a proper representation of the mechanical contraction [14]. Performing an echo scan is time-consuming and requires trained and skilled clinicians to record and interpret [15, 16]. There is furthermore a challenge in the relatively low temporal resolution of echo images, typically around 50 - 60 frames per second. This is, in some cases, too low to detect rapid changes in the cardiac contraction [17]. Further, the reproducibility of echo is challenging due to inter-operator variability both with regards to obtaining the images and analyzing them afterward.

Thus, this thesis investigates the method called seismocardiography (SCG), a non-invasive, easy to use, modality that can potentially assess cardiac mechanics. The SCG can be easily recorded with a higher sampling frequency than echo and the signal has high reproducibility, with a stable signal over time [18].

2.3 The Seismocardiogram

As the heart contracts and forces blood into the pulmonary and systemic system and subsequently relaxes, it changes shape and moves in the thoracic cage. The valves of the heart open and close to allow the blood to flow in the right direction. All this causes vibrations that can be recorded non-invasively with an accelerometer on the chest of the subject [19]. The magnitude of this signal is in milli-g (g being the gravitational constant $9.82\mathrm{m}\cdot\mathrm{s}^{-2}$ [20, 21]). The accelerometer is often placed on the lower part of the sternum, just above

the xiphoid process. The vibration signal is deterministic and shares the same characteristics between subjects [18]. The micro-vibrations produce an acceleration signal that was first presented by Patric Mounsey in 1956 [19].

2.3.1 History of the Seismocardiogram

When Patric Mounsey first published his paper about the cardiac accelerations he was able to record he did not use the term "Seismocardiogram" [19]. Mounsey had borrowed an analog accelerometer by Robert V. Elliott, who had developed it for recordings of the ballistocardiogram (BCG) [22]. Inspired by the name ballistocardiogram, Mounsey called the method (and his paper) "Præcordial Ballistocardiogram". Mounsey strapped the large accelerometer directly to the subject's chest and was able to obtain the accelerations produced by the beating heart [19]. In contrast to the ballistocardiogram that describes whole body movement caused by the forces of the blood being pumped around in the large arteries, the SCG is a local recording of the vibrations from primarily the heart [19, 23]. Mounsey described, in detail, the signal that he was able to record from the subjects. Using both the ECG and PCG as a reference, Mounsey characterized the slopes of the signal and related these to the contraction and relaxation of the heart, the opening, and closing of the valves, and the shift in the position of the heart. Mounsey constructed a normal "præcordial ballistocardiogram" based on 20 healthy subjects. Besides describing signals from healthy subjects Mounsey also obtained recordings from patients with different heart diseases such as systemic and pulmonary hypertension, atrial septal defect, mitral stenosis, aortic, and tricuspid incompetence and stenosis and compared these recordings to the normal signal [19].

In 1961 Bozhenko published a paper entitled "Seismocardiography - a new method in the study of functional conditions of the heart" and thereby introduced the term "Seismocardiography" [24]. In 1964 Baevsky, Egorov and Kazarian published "Metodika Seismokardiografii" and Kazarian took part in the development of the first pick-up used for seismocardiographic recordings in space flight for the "Vostok-5" and "Vostok-6" flights [25].

Following a period of relative silence within the field researchers Salerno and Zanetti introduced the method in the USA in the 1990s [18, 26]. At the time Zanetti and Salerno were able to correlate cardiac timing intervals derived from the SCG with intervals derived from echocardiography [27]. This was a great leap forward for the method and other researchers became interested in the technology [28, 29]. At the start of the 1990s, Salerno and Zanetti heavily investigated the use of SCG in different settings. Especially the correlation between changes in the SCG and coronary artery disease (CAD) was explored [30, 31]. Exercise SCG was obtained from an impressive number of 1.221 patients with suspected CAD [32]. If the patients had an
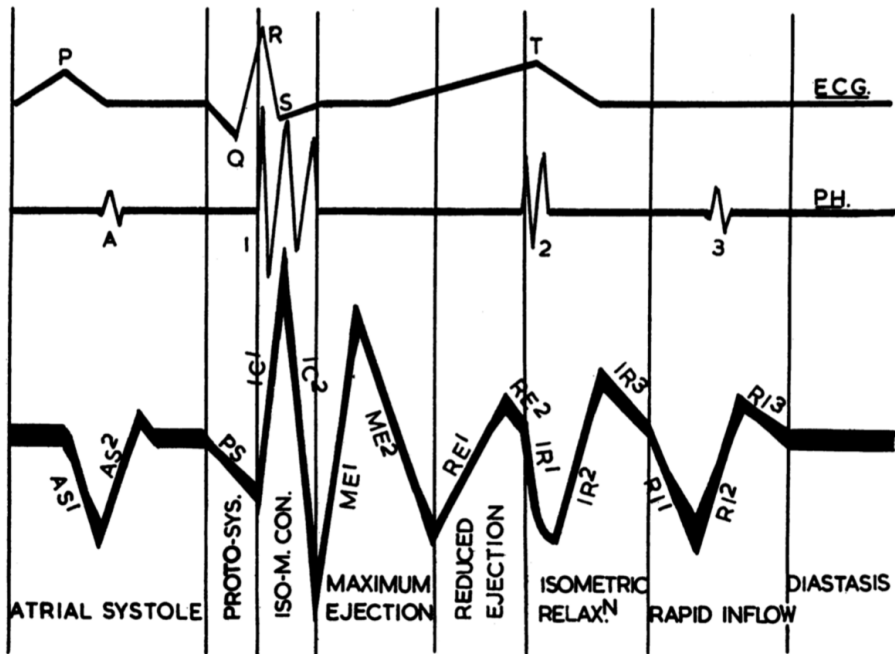
Fig. 2.4: Electrocardiogram (top), phonocardiogram (middle) and seismocardiogram (bottom) divided into eight periods: Atrial systole, protosystole, iso-volumetric contraction, maximum ejection, reduced ejection, iso-volumetric relaxation, rapid inflow and diastasis. The slopes are named according to the period in which the reside. ©Reprint with permission from BMJ, [19]

angiography within six months of the SCG recording they were included in the study and exercise SCG was obtained and analyzed to determine if it was normal or abnormal, according to a set of predefined criteria. The SCG had a sensitivity of 80% and specificity of 69% for the detection of CAD. In comparison, exercise ECG in the same study had a 67% sensitivity and 51% specificity, highlighting the advantage of the SCG [32]. The results were re-evaluated in a multi-center study with 129 patients. This study found, that inclusion of exercise SCG improved a prediction model for CAD [33]. In 2019, Dehkordi and co-workers published a paper with the data set obtained by Zanetti in 1988-92 [34]. Dehkordi developed two models for identification of CAD including more features from the SCG than originally by Salerno and co-workers [32, 33]. This improved the prediction model based on the exercise SCG to 82% and 84% sensitivity and specificity, respectively [34].

2.3.2 Recent Research

Since the early 2000s, there has been an increase in the number of publications concerning SCG. From 2000 to 2010 a range of 1-7 papers with the search term "seismocardio*" was included in the Scopus database per year. From 2010 to July 2020 this number was 4-59, peaking in 2020. The following section presents some of these publications and some of the results from these articles.

Cardiac Timing Intervals

Cardiac timing intervals (CTI) such as IVCT, left ventricular ejection time (LVET), mechanical systolic time, and IVRT can, with some success, be derived from the SCG due to the relative ease of identifying the mechanical events in the cardiac cycle [12, 18, 19, 27, 35, 36]. Thus, several of the studies evolving SCG, relate to different applications of use for the derived cardiac timing intervals, often as a surrogate for (or compared to) echocardiography. With the inclusion of a synchronous ECG signal more intervals can be derived, such as the pre-ejection phase (PEP) from Q-onset in the ECG to mitral valve closure in the SCG [37, 38].

In 2019 Dehkordi and co-workers published a study of 86 healthy subjects, comparing different methods for estimating cardiac timing intervals: SCG, PCG, and impedance cardiography (ICG) to ultrasound imaging [12]. This study shows promising results for the SCG and PCG methods compared to ICG for the estimation of cardiac timing intervals.

Pulse Transit Time and Blood Pressure Estimation

Because the opening of the aortic valve is seemingly well defined in the SCG (and the location of this event is coherent among most authors), the method is also used in the calculation of pulse transit time (PTT) with pulse plethysmography (PPG) sensor at the finger or earlobe [39–43]. Deriving PTT from SCG is of interest as it may provide a method for continuously estimating blood pressure (BP), eliminating the need for an acoustic-based BP monitor, such as the inflatable cuff [39, 42, 44, 45].

Yang and co-workers conducted a study on ten healthy male subjects, exploring how well different ways of estimating PTT derived from SCG and PPG would correlate to measured BP [39]. A logarithmic model with subjects specific parameters was used for the BP estimation. Correlations of the PTT derived from the SCG and the finger PPG were non-significant, with correlation coefficients ranging from 0.58 to 0.62 [39].

Continuously monitoring BP would be applicable in for instance the intensive care unit, for monitoring of critical patients. However, the results of the approach are varying with how good the estimation of the BP is, likely due

11

to the difficulty of modeling blood pressure, and the changes herein due to vasoconstriction and -dilation, only based on the pulse transit time [42].

Bi-ventricular Pacemaker Optimization

In 2007 Frank Marcus and co-workers published a paper where they investigated different cardiac timing intervals derived from the SCG signal in healthy subjects and patients submitted to cardiac resynchronization therapy (CRT) [46]. Marcus concludes that the SCG could be used for pacemaker optimization, as the CTIs change in the CRT patients, when turning on the pacemaker, indicating improved cardiac contractility. Further, the study showed a difference in the CTIs derived from healthy subjects and the patients [46].

Besides the non-invasive SCG recordings, accelerometers placed in the tip of pacemaker electrodes, like the SonR (MicroPort CRM, France) system are available [47, 48]. Mitral valve and aortic valve closure derived from the SonR have been shown to correlate well with those derived from echo [49]. The SonR system was developed to be used for pacemaker optimization, without the need for clinical consultation [15]. Studies show that the optimization proposed by the SonR system was as safe as the optimization proposed by a cardiologist [15].

Cardiac Performance Index

The CTIs derived from SCG has also been used for calculation of the Tei Index/Myocardial Performance Index with relation to exercise testing [29, 50, 51]. The Tei Index is calculated as the sum of IVCT and IVRT divided by LVET [52]. The index was developed as a combined index of both the systolic and diastolic time intervals as a predictor for overall ventricular dysfunction [52]. The method was developed using echo, but have since been evaluated using SCG [29, 50, 51]. In 2001 Libonati and co-workers derived the Tei Index from SCG and found that the Tei Index derived from the SCG correlated with exercise performance [50].

Wearable and Transportable Seismocardiography

The development of micro electro-mechanical systems (MEMS) accelerometers have provided a convenient way of measuring SCG. The first studies of the cardiac vibration signal was done with heavy equipment. For instance, the accelerometer used by Salerno and Wilson in 1992 weighed 1kg and was placed on the chest of the subject just after finishing a cycle ergometer protocol [32, 33]. One can imagine that this setup was probably not too comfortable for the test subject. The current lightweight accelerometer (weighing as little as 5 grams) can be attached to the skin with double adhesive, see Figure

4.1 [53]. The low weight ensures that the small vibrations on the chest are not obstructed. Further, applications for wearable SCG devices have been investigated [35, 54–56]. From November 2014 to June 2015 the "MagIC-Space system" was tested at the International Space Station as part of the "Wearable Monitoring Project" [57]. Di Rienzo and co-works recently published a paper describing their new system for monitoring daily life activities with the "SeisMote" system that is capable of recording SCG, ECG, and PPG [58].

Inan and co-workers developed an SCG and ECG sensing patch capable of more than 50 hours of continually recording [35]. The patch is attached midway between the xiphoid process and suprasternal notch and is capable of recording both SCG and ECG. Using the patch, standing resting SCG was compared to recovery SCG following a 6-minute walk test. With graph similarity score (GSS) based on features in the frequency domain of the SCG signal, Inan and co-workers were able to distinguish between compensated and decompensated patients with heart failure [35]. Shandhi and co-workers also used this wearable SCG and ECG path for estimation of VO_2 in both healthy and heart failure patients [59, 60].

Because of the relative ease of recording of the SCG, even the accelerometer in a modern smartphone can be used to record and process the signal in various settings, for instance for detection of acute myocardial infarction and atrial fibrillation, the latter have also been investigated with a normal MEMS accelerometer [61–63].

Automatic Segmentation and Fiducial Point Detection

In order to facilitate the usefulness of SCG, automatic segmentation and anno-tation/detection of the fiducial points in the signal is naturally an interesting research topic [64–74]. These approaches are different, ranging from using simultaneously recorded ECG to detect the R-peak first and then find the fiducial points in the SCG, over use of wavelets, to implementation of Hidden Markov Model.

2.4 Summary

Even though SCG seems promising in multiple clinical use cases, it never made it to the clinic and is still not used by clinicians [43]. This is most likely due to a combination of the complexity of the signal, the advancement of echocardiography and other image technologies and a lack of coherent nomenclature when defining the fiducial points in the signal [43, 56]. The latter becomes apparent when going through the literature. Most articles agree on the location that defines the mitral valve closure (MC), aortic valve

opening (AO) and aortic valve close (AC). Zanetti and Crow published the first papers with simultaneously SCG and echocardiogram recordings [27, 28]. The nomenclature introduced in these two papers have since been widely used when defining fiducial points, but there is still not complete agreement between authors, see Figure 2.5. The location of AC is different in all the figures. The MO location is the same in Figure 2.5a and 2.5d, but seems to be annotated late in 2.5b.

The ambiguity of the fiducial point locations, in combination with the promising clinical applications, lead to the aims of this thesis, presented in the next chapter.
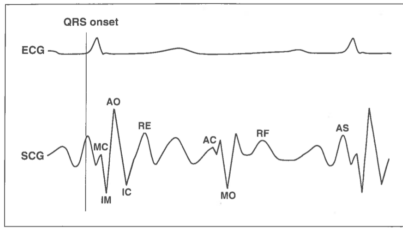
(a) ©Am J Noninvas Cardiol, Crow et al. [28]
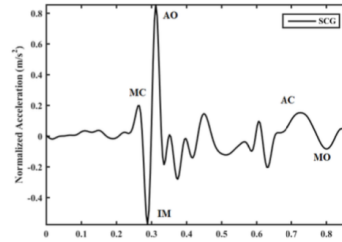
(b) ©IEEE Journal of Biomedical and Health Informatics, Yang et al. [75]
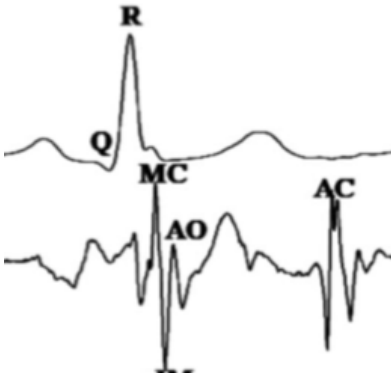
(c) ©IEEE Journal of Biomedical and Health Informatics, Khosrow-Khavar et al. [66]
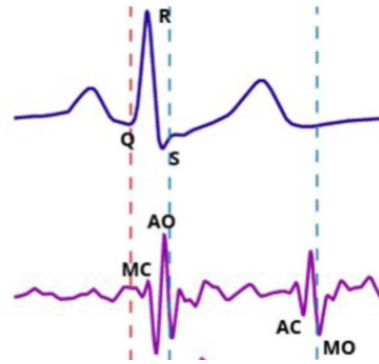
(d) ©Frontiers In Physiology, Dehkordi et al. [12]

Fig. 2.5: Seismocardiographic signals from four different articles. This illustrates the ambiguity between how authors label the signal

Thesis Aims

The following chapter describes the aims of the thesis.

The overall aim for the Ph.D. study was to gain a better understanding of the seismocardiogram and find clinical applications for the method.

When embarking on this Ph.D. thesis, the number of papers concerning seismocardiography was steadily increasing. At the time not many articles were describing the physiologic origin of the waveform of the signal. The nomenclature for the fiducial points was largely based on the studies by Zanetti, Salerno, and Crow [27, 28].

The first objective of this thesis was to investigate a cohort of normal healthy subjects in different age groups to describe the normal SCG signal. The goal of this study was to contribute to a greater understanding of how SCG signals manifest and how the fiducial points in the SCG correlates to physiologic events found in echocardiographic images. We hypothesized that certain fiducial points in the SCG would have a strong correlation and low temporal difference to the physiologic events found in the echocardiographic images.

The second goal of the thesis was to evaluate how the SCG signal recorded from patients submitted to CRT treatment would manifest. This patient group has been of interest to researchers previously and we hypothesize that SCG could be an easy and non-invasive way of optimizing the pacemaker settings. Current studies have primarily examined the CTIs derived from the SCG signals and neglected to examine visually how the signal changes and thus how the amplitudes of the signal changes when changing the settings of the bi-ventricular pacemaker [46]. We hypothesized that both the amplitudes of different segments in the SCG as well as some of the CTIs derived from the SCG will change between the different settings of the bi-ventricular pacemaker.

The third goal was to evaluate if the SCG could be used to access the cardiorespiratory fitness (CRF) level in healthy subjects. Cardiorespiratory

fitness is a combined measure of multiple physiologic parameters. In this explorative study, we hypothesized that either the derived cardiac timing intervals, the amplitudes of certain features in the SCG, or both would correlate with CRF determined by VO_2max.

Aims

To sum up, the three aims for the Ph.D. thesis were:

I Investigate and describe how the fiducial points in the normal SCG correlate with physiological events found in echocardiographic images

II Investigate how SCG recorded from patients submitted to CRT manifests and changes due to the treatment

III Evaluate if there is a correlation between features in the SCG signal and the cardiorespiratory fitness in healthy subjects

Methods and Materials

The following chapter describes the materials and methods used in the three thesis studies. A description of the accelerometers used throughout the studies and the general signal processing approach will be described. Methods specific to the studies are described in the summaries of the studies in Chapter 5.

4.1 Accelerometers used for the Seismocardiographic Recordings

The accelerometer(s) that should be used for the SCG recordings need to be sensitive enough to record the small vibrations and have a low noise floor so the signal does not drown in noise. Based on previous studies the SCG signal has a typical peak-to-peak amplitude about ± 10 mg [20, 21, 56]. However, the signal is often presented with no labeling on the y-axis, making it a bit more difficult to exactly estimate the possible peak-to-peak amplitude. Thus, an assumption peak-to-peak amplitudes of 1 to 100 mg was chosen to obtain both small variations in the signal as well as avoid saturation. The frequency range of the signal is not well-defined. Some papers report only the non-audible low-frequency band (0-25 Hz) while others include frequencies > 25 Hz [21]. For the studies in this thesis we wanted to be able to extract some higher frequencies from the signal as well (> 25 Hz) for use in our signal processing approach, see Section 4.2.3 for more details. Thus a frequency band of 0 to 80 Hz was chosen. We accept a root mean squared (RMS) signal to noise ratio (SNR) of 2. Thus for a signal of 1 mg, we allow the noise to be 0.5 mg. Based on the formula for noise calculation this yields a noise density of $56 \mu g / \sqrt{\text{Hz}}$, see Equation 4.1.

$$
\begin{aligned}
\text{Noise Density} &= \text{Noise}/\sqrt{\text{Band width}} \\
&= 0.5 \text{ mg}/\sqrt{80\text{Hz}} \\
&\approx 56 \ \mu g/\sqrt{\text{Hz}}
\end{aligned}
\tag{4.1}
$$

Based on the requirements listed above two accelerometers were chosen. The specifications for these are listed below.

Silicon Designs 1521-002

The 1521-002 is a MEMS accelerometer with a range of ± 2 g, a frequency response of 0-300 Hz minimum at 3 dB and a low noise floor at 7 μg/$\sqrt{\text{Hz}}$ [76]. This accelerometer was used in Study I and III.

Colibrys SF1600S.A

The SF1600S.A is a MEMS accelerometer has a range of ± 3 g, a frequency response of 0-1500 Hz minimum at 3 dB and low noise floor at 0.3 μg/$\sqrt{\text{Hz}}$ [77]. This accelerometer was used in Study II.

Both accelerometers have a lower noise floor than desired. The Colibrys accelerometer has a very low noise floor which we considered an advantage when recording the SCG from the HF patients, as these patients might have a weaker heart and thus a smaller recordable acceleration signal.

The data acquisition boxes used in the studies are from iWorx and have a resolution of 16-bit. This yields a resolution of 4 g$/2^{16}$ bit $= 0.06$ mg/bit for the Silicon Designs and 6 g$/2^{16}$ bit $= 0.09$ mg/bit for the Colibrys accelerometer. In both cases this is well below the desired lowest amplitude we want to obtain of 1 mg. Based on the Equation 4.2 the total RMS noise is calculated for the Silicon Designs accelerometer.

$$\begin{aligned} \text{Noise} &= \text{Noise Density} \cdot \sqrt{\text{Band width}} \\ &= 7 \ \mu\text{g}/\sqrt{\text{Hz}} \cdot \sqrt{80\text{Hz}} \\ &\approx 62 \ \mu\text{g} \end{aligned} \tag{4.2}$$

Using the same equation the total noise for the Colibrys accelerometer is 2.7 μg. Thus, noise introduced by the accelerometer itself is small compared to the signal we want to record (1000 μg). The SNR is 11 dB and 24 dB for the Silicon Designs and the Colibrys accelerometer respectively. Further, the signals will be divided into individual beats to calculate a mean SCG beat, see Section 4.2. This averaging approach will reduce the noise in the signal.

For both accelerometers, custom housing was 3D printed in ABS plastic making them easy to attach to the skin with double-sided adhesive while being electrically isolated from the subject, see Figure 4.1. A thin flexible wire with outer shielding was used for power and data transfer to and from

the accelerometers. The combination of the lightweight accelerometer and plastic housing brought the weight of the package to approximately 5 grams in total, without accounting for the wire. The housing is approximately 19 mm wide, 21 mm long and 11 mm high, see Figure 4.1. The Silicon Designs accelerometer was soldered onto a custom circuit print board that was then glued into the plastic housing. The circuit board was used to break out the pins from the MEMS accelerometer chip to the electrical wire for power and data transfer. The Colibrys accelerometer was supplied on a print board, that was glued into the housing.

Fig. 4.1: Example of one of the accelerometers used in the studies (yellow plastic housing), the power supply, filter and amplifier sleeved in black and the DIN8 plug.

Power Supply, Filter and Amplification

For both the Silicon Designs and the Colibrys accelerometer a custom power supply, filter, and pre-amplifier were constructed. The filter was designed with a high-pass cutoff at 0.3 Hz and a low-pass cutoff at 80 Hz (3 dB dampening). Power and data signal to and from this small circuit board was provided via a DIN8 plug, that fits the iWorx data acquisition units used for data sampling in the thesis studies.

Accelerometer Placement

The seismocardiographic recordings in the thesis papers were all done in the same location, the xiphoid process, see Figure 4.2. ECG electrodes were applied on the right and left shoulder as well as the right and left iliac crests to obtain a three-lead ECG signal. Besides the accelerometer for the SCG recordings, an accelerometer or microphone was used to record heart sounds,

placed in the 4th intercostal space (IC4). The use of the heart sound signal is described in Section 4.2.
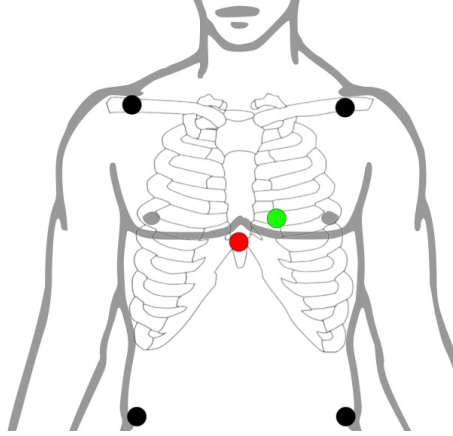
Fig. 4.2: Illustration of the placement of electrocardiogram electrodes (black circles), accelerometer for seismocardiographic recording on xipoid process (red circle) and accelerometer/microphone for heart sound recording in intercostal space 4 (green circle) [78]

4.2 Signal Processing

Throughout the studies in this thesis the term "mean beat" is used to describe one ECG, SCG, and/or PCG beat, constructed from a number of temporally aligned individual beats from a continuous recording. This section describes the signal processing pipeline that was used to process the initial recording, resulting in one mean beat.

For all recordings obtained as part of the studies both ECG and SCG were recorded simultaneously. Further, a PCG signal was recorded simultaneously as well using either a microphone or an accelerometer. The use of the PCG signal is described in detail in Section 4.2.3. The segmentation process of the raw signals can be divided into three main steps:

1. Detect R-peaks in the ECG for segmentation of the whole signal into individual beats

2. Use the location of the R-peaks to divide the SCG and PCG signals into individual beats

3. Using the heart sound signal for alignment of the individual beats

In all studies, the ECG was used as the reference for this beat segmentation approach. The approach was first described by Jensen et al. [79] and further by Sørensen et al. in Thesis Paper I [53]. All signal processing was performed in MATLAB versions 2016A to 2019B.

4.2.1 ECG R-peak Detection

In general, the approach applied to detect R-peaks in the ECG consists of multiple peak detections in small sections of the signal (windows), followed by peak detection in a version of the signal, with a different filter setting. This approach was found to be robust when introducing new and noisy signals to the algorithm.

The first step of the R-peak detection was to filter the raw ECG signal to remove 50Hz noise. This was done with an Infinite Impulse Response (IIR) Comb Notch filter at 50Hz. This ensured the removal of both the 50Hz noise and harmonic effects thereof, see Figure 4.3(B). Any global off-set was removed, by subtracting the mean of the signal, from the signal itself.
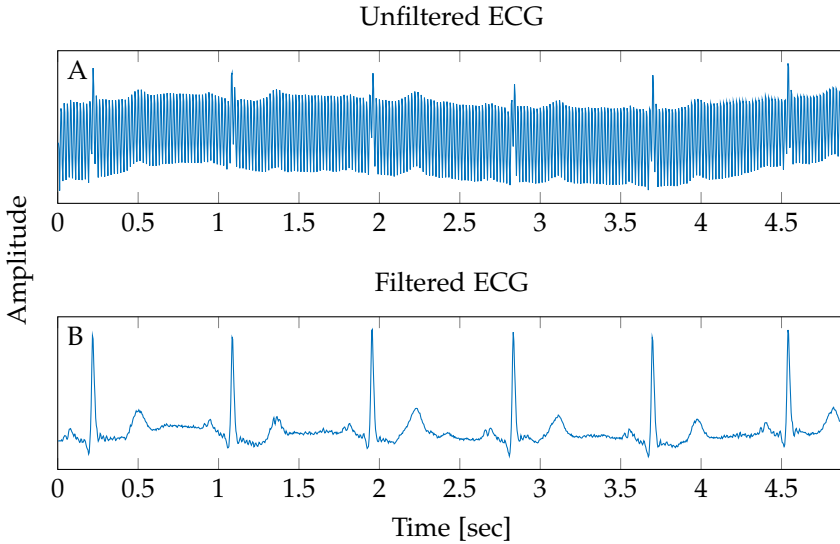
Fig. 4.3: Panel A: Typical example of an electrocardiogram that is polluted with 50Hz noise. Panel B: Same electrocardiogram after filtering with IIR Comb Notch Filter at 50Hz.

With most of the 50Hz noise removed, the next step was to detect peaks in the ECG signal. The ECG was inverted (amplitude multiplied by -1) and high-pass filtered with a 1st order high-pass filter at 2Hz to remove drift (for instance caused by respiration) and other very low frequencies in the signal.

Using the filtered signal the autocorrelation was computed and the left side of this was removed, keeping only positive lags. The largest peak of the autocorrelation in a predefined window of 600 to 2000 ms was used as a rough estimate of the periodicity of the ECG signal.

The inverted ECG was filtered with a band-pass filter (10 and 35Hz, 2nd order Butterworth) to emphasize the R-peaks and remove P- and T-waves, see Figure 4.4. Working on the inverted ECG was done to prevent the detection of the T-wave in some rare cases where the filter was not able to remove it. Using the estimated period from the previous step, a window with the length of 120% of the period was moved across the inverted, filtered ECG in steps of a quarter of the window size, illustrated as the red squares in Figure 4.4.
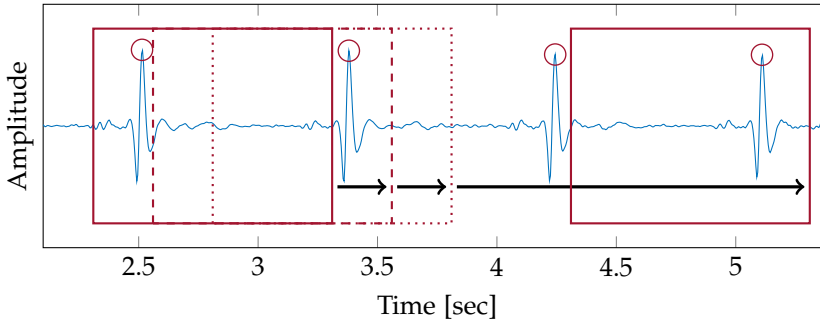
Fig. 4.4: Inverted and band-pass filtered ECG (10 to 35Hz) in blue. The red squares illustrate the search window, that was moved across the signal. Circles indicating the local maxima found in each window.

In each window-step, the maxima was detected, see the circles in Figure 4.4. The location of the peaks was used to find peaks in a second separate, independently band-pass filtered version of the inverted ECG signal (1 to 40Hz, 2nd order Butterworth). This is illustrated in Figure 4.5. The blue signal is the signal from Figure 4.4, with the red squares representing the shorter search windows used in this step of the algorithm. In Figure 4.5(B) the green signal, is the filtered signal between 1 to 40Hz. In the search window, the maximum of the green signal is marked as the cross.

Figure 4.6(A) illustrates the search windows (red squares) for this step in the algorithm. The location of these windows is based on the peaks illustrated with the crosses. These peaks were found in the previous step, see 4.5. Figure 4.6(B) illustrates one of the windows. A third, independent, non-inverted ECG signal, filtered between 0.5 and 45Hz with a 2nd order Butterworth low-pass filter followed by a 1st order high-pass Butterworth filter is illustrated with the blue line, and the star marks the R-peak found as the global maximum in

that window.
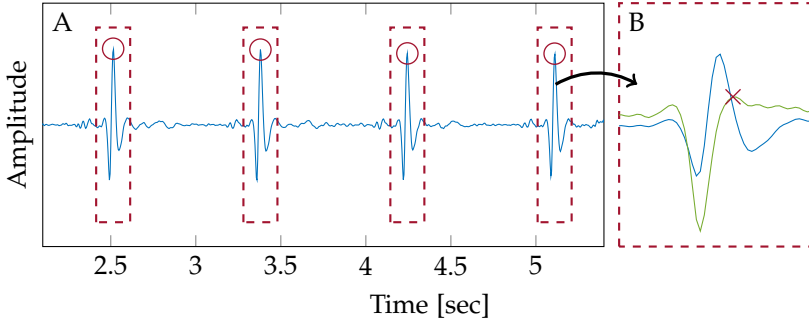
Fig. 4.5: Panel A: Inverted and band-pass filtered ECG (10 to 35 Hz) in blue. Illustration of the search windows (red squares) located based on the peak detection in Figure 4.4. Panel B: One search window from Panel A used to detect the peak, marked with the cross, in the green signal (independent, inverted ECG filtered 1-40Hz).
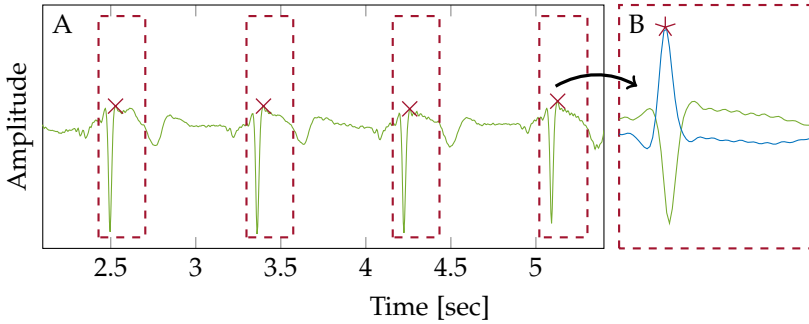
Fig. 4.6: Panel A: The inverted band-pass filtered signal (1-40Hz), from Figure 4.5(B) with the red squared indicating the search windows for this step. Panel B: One search window from panel A, with a non-inverted, filtered version of the ECG in blue. The red star marks the R-peak, found as the maximum in the search window.

The final result of the R-peak algorithm is illustrated, see Figure 4.7. In cases with peaks within 333 ms of each other both were removed as these were not considered R-peaks, because of the short RR-interval it would imply. Peaks with extremely high (twice as large as the median R-peak) amplitude were also removed.

The resulting R-peak locations were used to divide the ECG, SCG, and PCG signals into individual beats. Based on a predefined beat length (1.33 sec), segments of 25% (0.33 sec) of the beat length before the R-peak and 75% (1 sec) of the length after the R-peak were extracted.
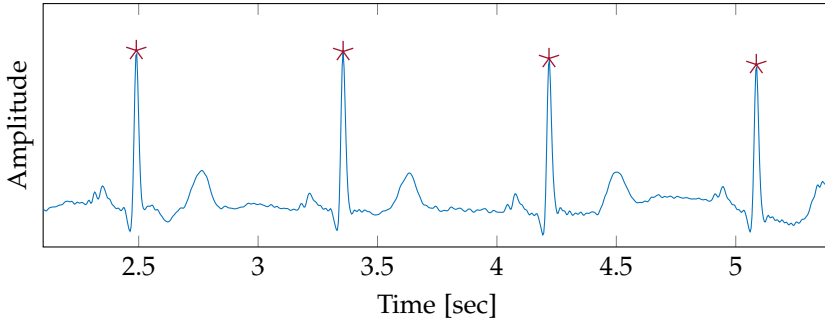
Fig. 4.7: ECG with the final location of R-peaks detected, marked with the red stars.

Removing Noisy ECG Beats

To reduce the number of noisy ECG beats, a segment from the individual beats in a window from 0.25 sec before to 0.5 sec after the R-peak were extracted, see the red squares in Figure 4.8. The sum of squared errors (SSE) between the individual segments and a median segment calculated from the individual segments were calculated. A threshold was computed as 2.5 times the 75th percentile of the SSEs and segments with a SSE larger than the threshold were discarded, see Figure 4.8.
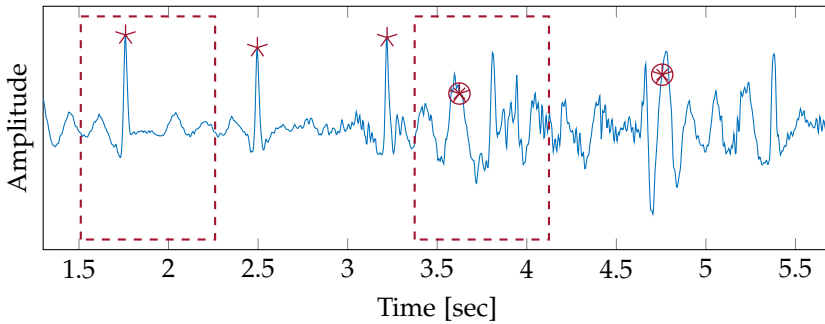
Fig. 4.8: An example of a part of a ECG signal containing two noisy beats and three normal beats. The red squares indicate two examples for the windows used for calculation of sum of squared error (SSE). The two last beats detected (illustrated by circles with a start in them) will be discarded as part of the segmentation algorithm due to too high SSE compared to the median beat.

4.2.2 Segmentation of the SCG Signals

The SCG signals were recorded simultaneously with the ECG signal. Based on the temporal locations of the R-peaks in the ECG, the continuous SCG signal (Figure 4.9 panel A) was divided into individual beats (Figure 4.9 panel B). From the individual SCG beats a mean SCG beat was computed (Figure 4.9 panel C). As with the ECG beats, the SSEs between the individual SCG beats and the median SCG beat were calculated. The threshold for discarding beats was calculated as 1.2 times the 75th percentile of the SSEs.
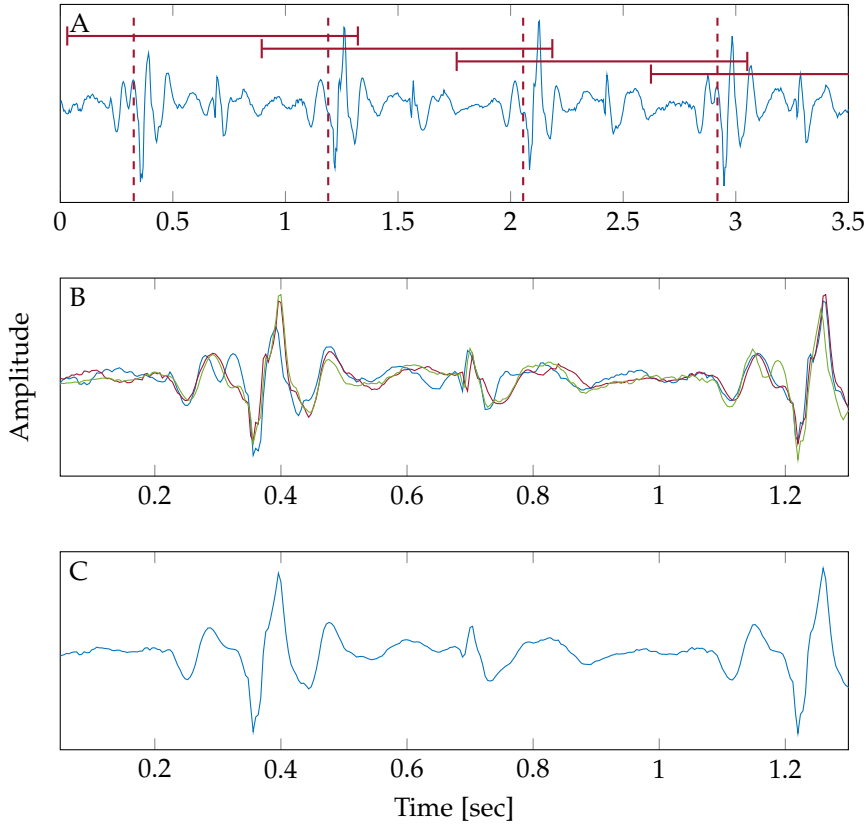
Fig. 4.9: An example of how a seismocardiogram (SCG) is segmented into individual beats, before calculating a mean beat. Panel A: part of a SCG signal. Red vertical lines indicate R-peak locations found in the ECG. Red horizontal lines indicate the length of the windows that were extracted. Panel B: Three of the extracted individual beats from panel A, plotted in different colors. Panel C: A mean beat calculated from the three beats in panel B.

In Figure 4.9 panel C all the individual beats are aligned based on the R-peak of the ECG. This can cause the characteristics of the signal to diminish,

especially in the diastolic phase of the signal, due to the natural variation in the cardiac contraction and relaxation, see Figure 4.10. Thus, the heart sound signal was used to re-align the individual beat, to the diastolic complex as well. This approach is described in the following section.
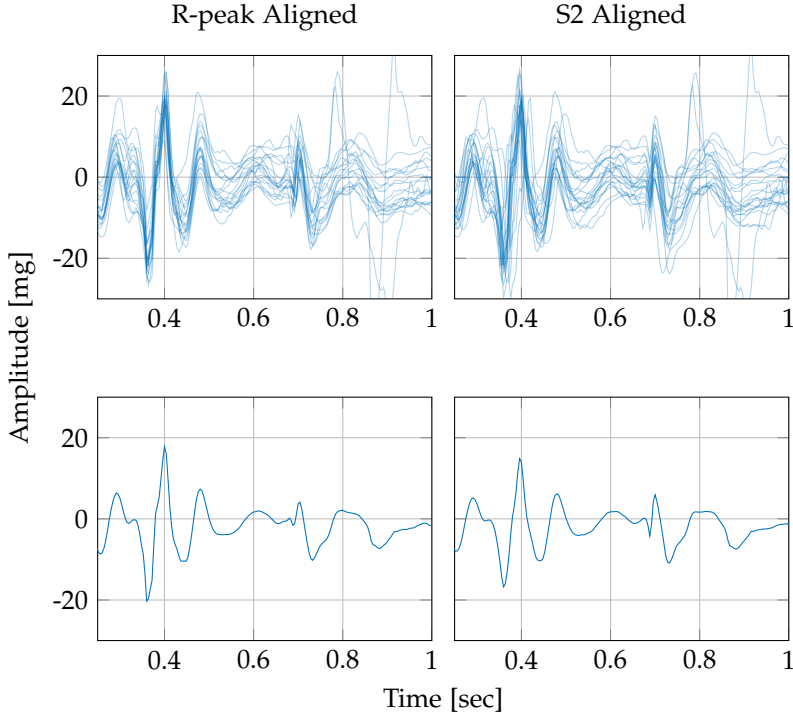
Fig. 4.10: The figure illustrates the difference in the seismocardiographic signal due to alignment. The same individual beats (n=20) are presented in both top plots. Individual beats are aligned to the R-peak to the left and the 2nd heart sound (S2) on the right. The bottom plots visualizes the mean beat, based on the individual beats. Note the difference in amplitude between the two alignments. Data and inspiration from [53].

4.2.3   Using Heart Sound Signals for Alignment

Besides the accelerometer placed on the xiphoid process, an accelerometer or a G.R.A.S 40AD microphone was placed in the IC4 for the recording of the heart sound. In Study II the G.R.A.S 40AD microphone was used and in study I and III a Silicon Designs 1521-002 accelerometer was used as a proxy for the microphone. This signal was used to align the individual beats to the first or second heart sound to avoid the signal distortion visualized in Figure 4.10.

The general idea behind this approach was to first detect an approximation

for the S1 and S2 location and then incrementally realign the individual beats to a median beat, recompute a new median beat and once again realign the individual beats to this new median beat. This approach realigns the individual beats by a few milliseconds.

The PCG signal was filtered with a band-pass Butterworth filter at 50 and 500Hz (both at 1st order) to remove lower frequencies (such as the SCG component of the signal) and emphasize the higher frequencies due to the valve closures. The signal was then divided into individual beats based on the ECG R-peaks as described in the previous section. From these, a median beat was calculated and the Hilbert transform was computed. Two peaks in the Hilbert transform were located, with a predefined minimum distance to each other, ensuring that two adjacent peaks in the S1 were not detected as S1 and S2, see Figure 4.11. These two peaks were considered as the initial S1 and S2 peaks for all the beats, regardless of the actual S1 and S2 location for the individual beats.
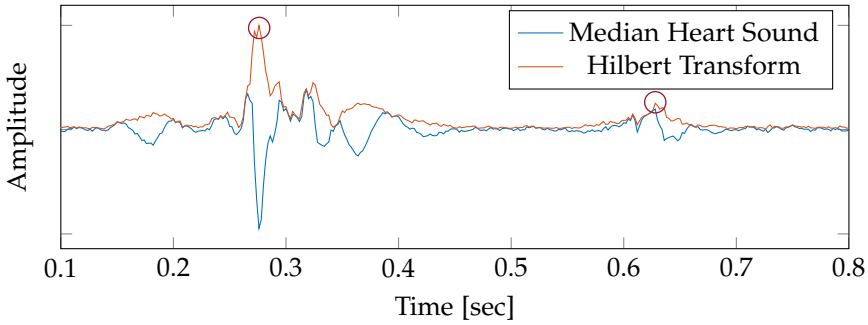
Fig. 4.11: Illustration of a median heart sound signal (blue line) and absolute values of the Hilbert transform (orange line). The circles indicate the two peaks found as the initial S1 and S2 peaks.

The Hilbert transform was calculated for all the individual beats, in windows around the S2 location. The maximum in each of the individual transforms was detected and the temporal distances from these individual maxima to the initial S2 maxima were calculated. These maxima were used as the peak of the S2 sound and new individual beats were extracted from the PCG signal, based on the location of the peaks. These individual beats were now slightly more aligned towards an overall S2 location.

Based on these, windows around the S2 were extracted and a median S2 sound was calculated and the lags resulting in the maximum cross-correlation between the individual and the median S2 sound were computed. Using the lags the individual beats were re-aligned again, see Figure 4.12. A new median S2 sound was computed and re-alignment using the cross-correlation lags was

performed once again. Thus, for the alignment to S2, three increments were performed.
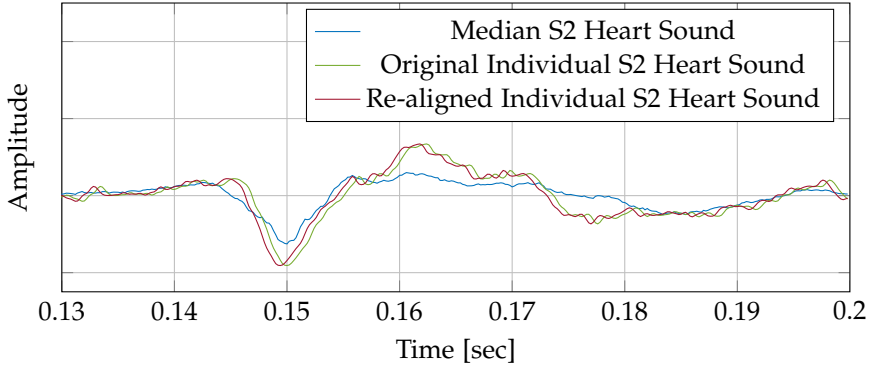
Fig. 4.12: Visual representation of alignment of individual S2 beats (green line) to the median (blue line) S2 sound (composed of 68 individual beats). The lag that resulted in the maximum cross-correlation between the median and the individual beat was used to re-align the individual beat to the median beat (re-aligned beat in red).

The approach ensured that the initial alignment of the individual beats to the R-peak and the initial S2 is omitted. Using the lags, both the SCG and PCG signals can be aligned to the S2 sound. When computing the mean with the individual beats aligned to S2, the characteristics in the diastolic complex are preserved (see Figure 4.10). Much like alignment to the S2 sound, the beats can be aligned to the S1 sound (using the initially found S1 peak in Figure 4.11). The only difference between the procedures is, that the Hilbert Transform is not computed and used for the initial re-alignment to S1, because the location of the S1 sound is located close to the R-peak. Thus, there is no need for at large re-alignment as in the case with the S2 sound.

With the algorithm described in the signal processing section, the mean beats used for the studies were calculated. The approach was slightly different for the R-peak detection in Study II, that involved patients with a Bi-Ventricular pacemaker, to make sure that the pacing spikes were not detected as R-peaks.

Summary of Thesis Studies

The following chapter will contain summaries of the three thesis studies. Results from the studies are documented in the papers, available as appendices in the full version of the thesis. Discussion of the three studies are found in Chapter 7.

5.1   Study I

The first study was carried out to fulfill Aim I:

Investigate and describe how the fiducial points in the normal SCG correlate with certain physiological markers found in echocardiographic images

The results from the study are published in Thesis Paper 1: "Definition of Fiducial Points in the Normal Seismocardiogram" [53] as well as in the conference abstract "Seismocardiographic correlations to age, gender and BMI" [80].

Introduction

At the time of conducting the study, no article existed that thoroughly examined all the fiducial points in the SCG and correlated these with physiological events found from echocardiographic images. The definition of the fiducial points and their relation to physiological events in the cardiac cycle was (and still largely is) based on the work by Zanetti, Salerno, and Crow from the 1990s [18, 26–28]. The papers that were published at the beginning of the 1990s did not refer to the article written by Patric Mounsey, who had already described the SCG signal in great detail, see Section 2.3.1 [19]. Instead, the articles showed the SCG signal together with the ECG overlaid on echo images, to get a visual representation of the temporal correlation between the three.

A large review, published in 2015, of recent advantages of SCG and BCG, written with input from the major researchers within the fields, it became evident that even though we know a lot about the SCG signal - it is still not

fully understood [43]. Especially, there is not a coherent labeling of fiducial points.

To gain a better understanding of the signal in general, this study was designed to objectively correlate all prominent peaks and valleys in the SCG signal, to physiologic events found in echocardiographic images.

Methods

Forty-five healthy subjects were recruited in three age groups, 15 subjects in each group: 20-40 years, 40-60 years, and 60-80 years. The study was approved by the scientific ethical committee of Northern Jutland (N-20120069). All subjects signed written informed consent before participating in the study. Subjects were free of known cardiac diseases.

Resting three-lead ECG, PCG and SCG were recorded, the latter with low weight, high sensitivity accelerometers (see Section 4.1 for more information about the accelerometers used in the study), with the subjects in a supine position. One accelerometer was placed just above the xiphoid process for obtaining the SCG signal and one accelerometer was placed in the IC4 for the recording of heart sound, see Figure 4.2. An iWorx IX/228 Data Acquisition System was used to record the signals at 5000 Hz. SCG, PCG, and ECG were recorded for 5 minutes, using only the last 3 minutes for the signal analysis.

Using a GE Healthcare Vivid E9 ultrasound scanner, apical 4 and 5-chamber Pulsed Wave Doppler (PWD) and M-mode Tissue Doppler Images (TDI) of the mitral valve leaflets were obtained. The electrodes from the Vivid E9 was placed next to the electrodes used to record the ECG for the iWorx setup.

Mean SCG beats were calculated as described in Section 4.2. A custom tool was developed in MATLAB 2019a for visualizing the signals. All prominent fiducial points in the SCG mean beats were manually annotated using the MATLAB tool. This process was iterative, to ensure that the fiducial points from the different subjects, were annotated in the same way. The fiducial points were annotated by one operator and then validated by another operator. For transparency, all the signals with the fiducial points are uploaded along with the published article from the study [53].

In the echo images, physiologic events were annotated and the temporal distance to the R-peak of the ECG tracing on the bottom of the image was registered, using the free software HOROS. In the pulsed wave doppler 4-chamber images, the E and A wave were annotated, corresponding to the early diastolic phase and the atrial contraction, respectively [11]. Both the beginning and the peak of the waves were annotated to correlate all events to the SCG fiducial points, see Figure 5.2. In the 5-chamber images, the profile of the outflow of the left ventricle was traced, annotating the onset, the peak,
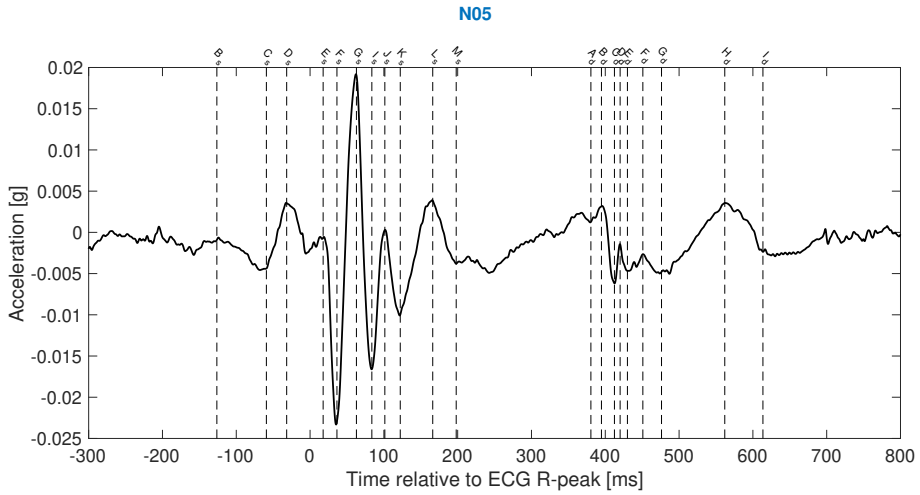
Fig. 5.1: An example of a seimocardiographic signal (from subject N05). All prominent fiducial points in the signal are annotated. ©Scientific Reports Reprint with permission from [53] (supplementary material).

and end, see Figure 5.3. The start of this is correlated to the beginning of the opening of the aortic valve [11]. With the M-mode tissue doppler images, mitral valve opening, and closing together with aortic valve opening and the closing were annotated, see Figure 5.4 [81]. To ensure consistency in the annotation of the physiologic events, two operators were assigned to annotate the images. In the case of temporal difference of > 15ms between operators, the location of the event was reevaluated. Averages of the temporal locations of the events between the two operators were calculated and used in the data analysis. If the echo image contained more than one beat, all beats were annotated and average temporal locations were derived. Synchronization between the image and the ECG leads of the Vivid 9 was examined and found to be less than one frame (70 frames/sec acquisition).

Physiologic events found in the echocardiographic images were correlated to all the fiducial points in the SCG using the Pearson Correlation. The distance from the R-peak of the ECG to all the events was calculated as well.
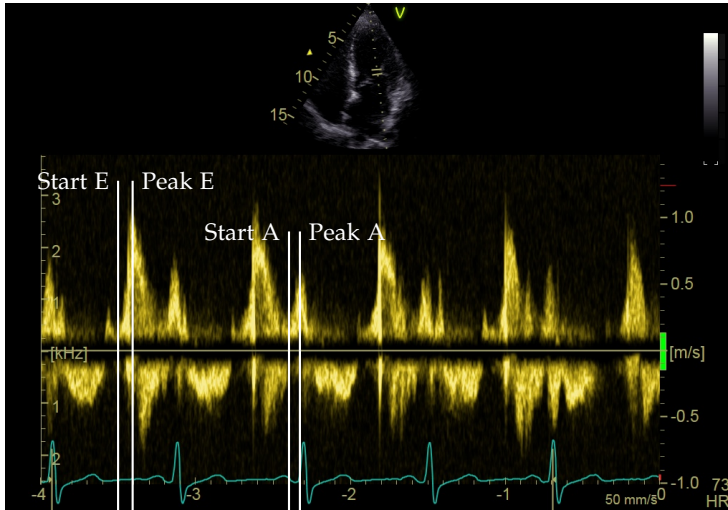
Fig. 5.2: Pulsed Wave Doppler echocardiographic image from a participant of the study (N24). Start and peak of the E (early diastolic phase) and A (atrial contraction) is annotated with the white vertical lines.
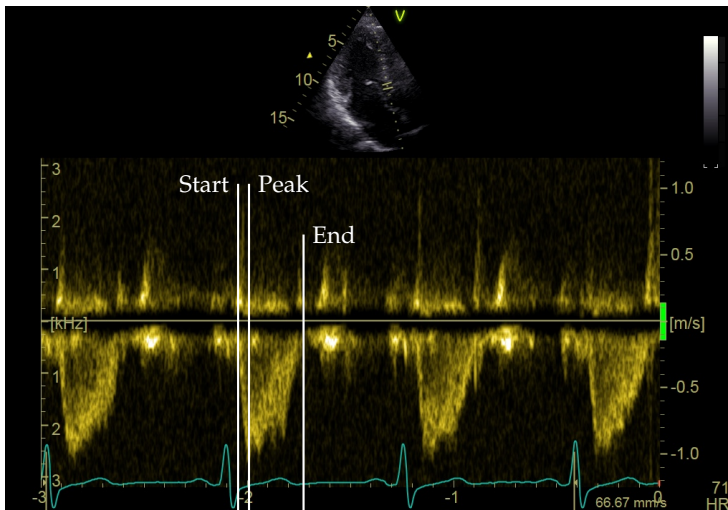
Fig. 5.3: Pulsed Wave Doppler echocardiographic image from a participant of the study (N24). Start, peak and end of the blood flow out of the ventricle is annotated with the white vertical lines.
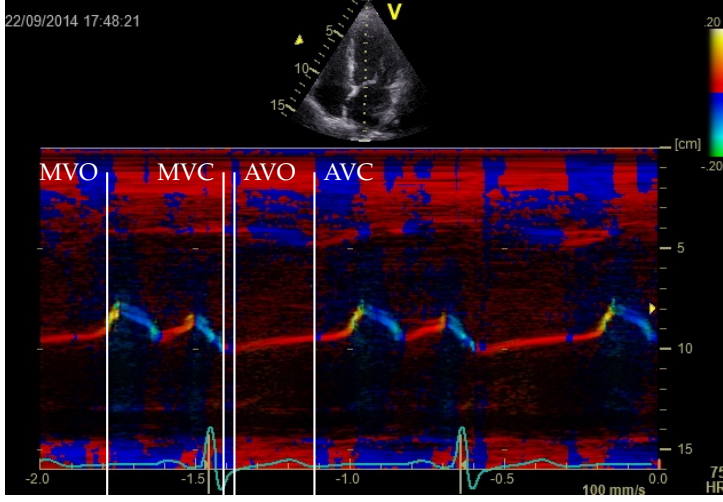
Fig. 5.4: M-mode tissue doppler echocardiogram from participant of the study (N24). The white vertical lines indicate the four physiological events: mitral valve opening (MVO), mitral valve closure (MVC), aorta valve opening (AVO) and aorta valve closure (AVC) is annotated with the white vertical lines.

Results

A total of 45 subjects participated in the study, of which one subject decided to withdraw. Two subjects were excluded due to abnormal SCG signals with unidentifiable fiducial points. In the SCG, we identified eight common fiducial points with a short temporal difference and high correlation, to the events found in the echo images. The eight physiologic events derived from the echo images were: atrial systole, peak atrial inflow, mitral valve closure, aortic valve opening, peak systolic outflow, aortic valve closure, mitral valve opening, and early ventricular filling. An overall mean ensemble SCG signal, based on all the signals included in the study was computed to visually illustrate the locations of fiducial points and their corresponding physiologic event, see Figure 5.5.

Conclusion

This study investigates and describes the foundation of the SCG with reference to echocardiographic images. The study contributes to the overall understanding of the SCG signal and gives a frame of reference that can be used by other researchers within the field of SCG. For the fiducial points E_s, G_s and B_d our findings are similar most other research papers. The location of F_d (correlated

to the mitral valve opening) that we found is not commonly annotated in this location by other researchers.

The results from the study have been used as a framework for reference when defining fiducial points in Study II and III.
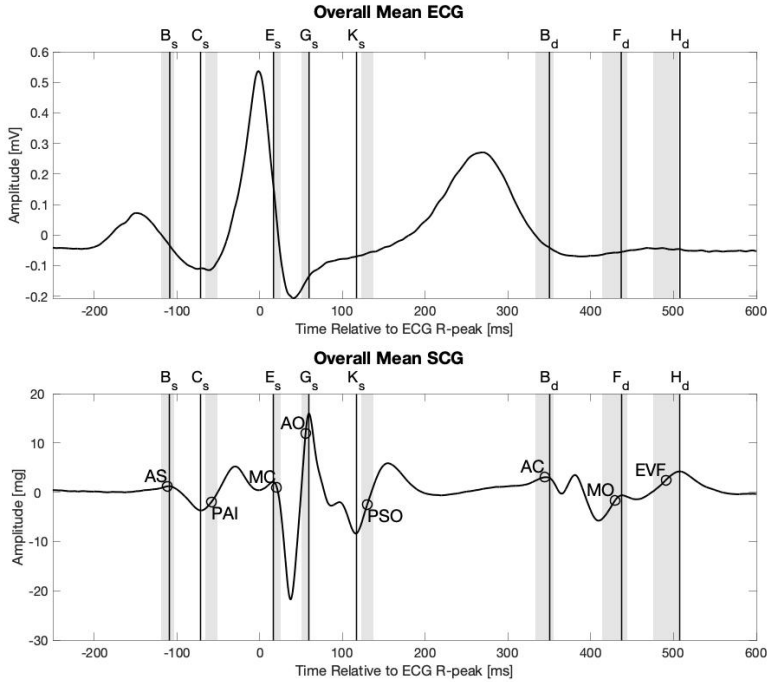
Fig. 5.5: Overall mean electrocardiogram and seismocardiogram based on the subjects included in study I with the eight physiologic events and corresponding fiducial points. Atrial systole (AS), peak atrial inflow (PAI), mitral valve closure (MC), aortic valve opening (AO), peak systolic outflow (PSO), aortic valve closing (AC), mitral valve opening (MO), early ventricular filling (EVF). 95% confidence intervals of the mean locations from the ultrasound image are marked in grey, with the circles indicate the mean of these locations. ©Scientific Reports Reprint with permission from [53]

5.2 Study II

The second study was carried out to fulfill Aim II:

Investigate how SCG recorded from patients submitted to CRT treatment manifests and changes, due to the treatment

The results from this study are documented in the Thesis Paper 2: "Seismo-cardiography as a Tool for Assessment of Bi-Ventricular Pacing" and in the conference abstract "Changes of Seismocardiographic Intervals in Cardiac Resynchronization Therapy" [82].

Introduction

Following the first study with healthy subjects, we wanted to examine the SCG signal from patients with heart failure (HF), to investigate cases with "abnormal" SCG signals. This was done to gain insights into the change in morphology of the signal compared to normals and to investigate potential clinical use for the SCG method.

Left bundle branch block (LBBB) is one type of heart failure. A blockage in the left bundle of the electrical conduction system of the heart impairs the normal synchronous contraction of the heart, leading to slow pressure rise in the left ventricle (dP/dt_{max}) [14, 83]. If the contraction of the two ventricles is not in sync the late activation of the left ventricle can push the non-activated septum wall towards the right ventricle, resulting in poor stroke volume [14]. LBBB is recognized in the ECG as a QRS complex duration of more than 120 ms. Wide QRS complex occurs in about 25% of all HF patients and is associated with a 1.7-fold higher risk of sudden death [14, 84]. The treatment for LBBB can be cardiac resynchronization therapy (CRT) [14]. A pacemaker device is implanted with three electrical leads positioned in the myocardium. Leads are implanted in the right atrium, right ventricle, and left ventricle. The right lead is positioned high in the atrium and the lead in the right ventricle, near the apex of the heart [85]. The left lead is commonly positioned in the lateral wall midway between the base and the apex of the heart [85]. The leads are used to stimulate the contraction of the heart, to improve the synchronization of the ventricular contraction. This should in turn improve dP/dt_{max} and stroke volume [84]. CRT has been shown to improve quality of life, reduce hospitalization, improve exercise tolerance and oxygen uptake and reduce mortality [83–88]. For the CRT to be effective, the delay between the electrical activation of the pacing leads needs to be optimized. This can be done based on the maximization of stroke volume measured with echocardiography. However, evidence of the technique is lacking and there is no consensus whether this is the best way to optimize the pacing delay [89].

Thus, we wanted to explore how the SCG signal from patients with CRT devices manifests and how it changes due to CRT. If there is a measurable change in the signals, SCG might be used as a tool for pacemaker optimization in the future. Examples of this have been investigated with promising results with the SonR system (accelerometer in the tip of the implanted pacemaker lead) [15, 47, 48] and in a previous study with SCG performed by Frank Marcus and co-worker [46].

Methods

Much like the study by Marcus from 2007, we recruited patients with a CRT device implanted and recorded resting SCG and ECG both with the pacemaker turned off and in bi-ventricular pacing mode [46]. A blanking period of 2 minutes was allowed between the two settings. Signals were recorded for a minimum of two minutes, and the signals were divided into individual beats, before calculating a mean beat for each patient, as described in Section 4.2. Besides the SCG signals, echocardiography was used as a reference modality for obtaining cardiac timing intervals. The modality was also used by a clinician to determine if the pacing delay was optimized to achieve maximum cardiac output.

The study was approved by the local scientific committee of Northern Jutland, Denmark (N-20160068) and participants signed written informed consent before participating in the study.

Using the framework from Study I, the following fiducial points were located in the SCG signals: E_s, F_s, G_s, J_s, and K_d in the systolic complex and B_d, C_d, and D_d in the diastolic complex. A high frequency filtered heart sound signal was used to guide the annotation of E_s and B_d (commonly referred to af MC and AC). Based on the fiducial points, iso-volumetric contraction time (IVCT, from E_s to G_s), iso-volumetric relaxation time (IVRT, from B_d to F_d) and ejection time (from G_s to B_d) was calculated. Further, alternative time intervals for IVCT and LVET was derived, using the J_s fiducial point as indicator for the AO. Peak-to-peak amplitude from F_s to G_s (Systolic Amplitude 1), G_s to I_s (Systolic Amplitude 2) as well as B_d to C_d and C_d to D_d was computed. The amplitude between the maximum and minimum signal amplitude, in the interval between E_s and K_s was also determined.

The cardiac timing intervals and amplitudes were compared between the two pacemaker settings with the Student's t-test and Wilcoxon Sign Ranked test respectively, the latter due to the non-normally distributed nature of the amplitudes. The timing intervals and amplitudes were compared with a two-sample t-test and Mann-Whitney U-test to a subgroup from the healthy subjects from Study I. This subgroup consisted of 14 subjects with a mean age of 64 ± 4 years. Pearson's correlation and the temporal difference between

the timing intervals derived by SCG and echocardiograms were calculated.

Results

A total of 19 patients were recruited for the study and 14 were included in the final data analysis. For five patients it was assessed, by the clinician, that turning off the pacemaker would be harmful to the patient. The patients had a mean age of 61.1 ± 11.9 years. For all patients, an improvement in LV ejection fraction was observed within one year of CRT implantation. Figure 5.6 is an example of two SCG signals from the same patient, with the bi-ventricular pacemaker turned off and on. The amplitudes are generally larger and the signal has a better resemblance to that of a normal SCG with the pacemaker turned on (see Figure 5.5 for reference).

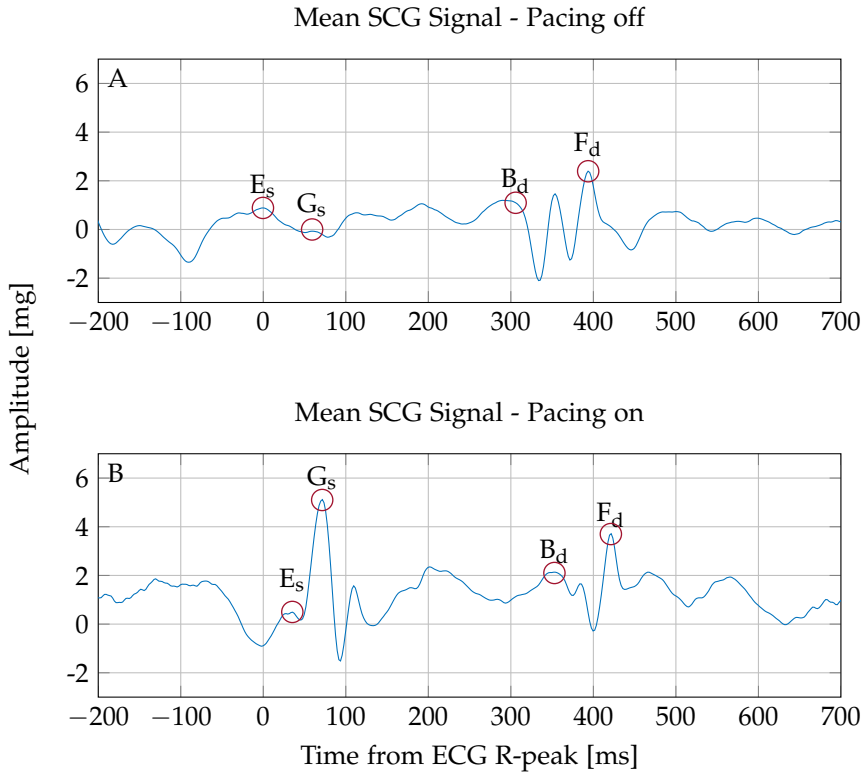**Fig. 5.6:** Mean SCG signals for the same patient. Panel A: Bi-ventricular pacer turned off. Panel B: Bi-ventricular pacer turned on. Fiducial Points E_s (correlated to mitral valve closure), G_s (correlated to aortic valve opening), B_d (correlated to aortic valve closure) and F_d (correlated to mitral valve opening) is marked in the red circles. Note that the scaling on the Y-axis is the same in the two panels.

The IVCT was significantly shorter with the bi-ventricular pacemaker turned on compared to off (52.6 ± 14.4 ms compared to 63.2 ± 20.9 ms, p = 0.027). The Systolic Amplitude 1 was significantly larger with the pacemaker turned on compared to off (8.8 ± 9.0 mg compared to 4.7 ± 3.5 mg, p = 0.002). The |max-min| amplitude in the systolic complex was larger with the bi-ventricular pacemaker turned on as well (9.8 ± 9.1 mg compared to 6.1 ± 4.4 mg, p = 0.003). There were no significant changes to the two other timing intervals nor the three other amplitudes. IVCT derived using J_s as the indicator for AO was also significantly shorter with the bi-ventricular pacer turned on as well (92.9 ± 12.5 ms compared to 111.9 ± 18.9 ms, p = 0.009).

When using the two fiducial points G_s and J_s as reference for AO, correlations and the temporal difference between the timing intervals derived from SCG and echo changes, see Table 5.1. With bi-ventricular pacing turned on, the correlation is highest when using G_s as reference for AO. The temporal difference, however, is shorter using J_s. With the bi-ventricular pacemaker turned off, the correlation for IVCT if highest when using J_s as reference for AO. The temporal difference is still shortest using J_s as an indicator for AO.

	Pacing ON		Pacing OFF	
G_s for AO				
	Rho (p)	Difference [ms] Mean (± SD)	Rho (p)	Difference [ms] Mean (± SD)
IVCT (n = 14)	0.63 (.015)	27.2 (± 14.8)	0.46 (.098)	45.4 (± 24.6)
LVET (n = 14)	0.72 (.004)	-23.0 (± 25.4)	0.66 (.01)	-65.0 (± 38.4)
J_s for AO				
	Rho (p)	Difference [ms] Mean (± SD)	Rho (p)	Difference [ms] Mean (± SD)
IVCT (n = 13)	0.46 (.117)	-13.2 (± 17.8)	0.79 (.001)	-2.2 (± 16.5)
LVET (n = 13)	0.58 (.036)	15.7 (± 31.2)	0.55 (.054)	-18.0 (± 42.3)

Table 5.1: Pearsons Correlation and temporal difference between timing intervals derived from seismocardiogram and echo cardiogram, using the two fiducial points G_s and J_s as indicator for aortic valve opening (AO). P-values for Pearsons Correlation is presented in parenthesis.

Comparing the cardiac timing intervals and the amplitudes to the subset of healthy subjects from Study I showed that all amplitudes were significantly smaller for the CRT patients. IVCT was significantly longer in the CRT patients with the pacemaker turned off compared to the healthy subjects. The difference was non-significant with the pacemaker turned on. IVRT was significantly shorter for the CRT patients (bi-ventricular pacing turned on and off) compared to the healthy subjects.

For the healthy subjects IVCT and LVET derived from SCG had a correla-

tion to echo of 0.90 (p < 0.001) and 0.92 (p < 0.001) with a temporal difference of -2.2 $\pm$ 6.5 ms and -1.3 $\pm$ 14.1 ms, respectively. Using the J_s fiducial point for the indication of aortic valve opening resulted in a larger temporal difference between timing intervals (-38.1 ms for IVCT and 44.7 ms for LVET) but the correlation was still significant for both (0.71 for IVCT and 0.97 for LVET).

Conclusion

It is possible to detect changes in the cardiac timing intervals and amplitudes derived from the SCG signal in patients with a bi-ventricular pacemaker. Two amplitudes derived from the SCG was significantly larger with the pacemaker turned on compared to off. IVCT derived from SCG was shorter with the pacemaker turned on compared to off. The method could potentially be used to assess the effects of CRT treatment but further research is needed, to determine why the temporal difference and correlation vary between the modalities dependent on the pacemaker setting.

5.3   Study III

The third study was conducted to fulfill Aim III:

Evaluate if there is a correlation between features in the SCG signal and the cardiorespiratory fitness in healthy subjects

The results of this study are published in the article "A Clinical Method for Estimation of VO$_2$max Using Seismocardiography" [78] and in the conference abstract "Correlation between Valve Event Amplitudes in the Seismocardiogram and VO$_2$max" [90].

Introduction

In 2016 the American Heart Association (AHA) published a clinical statement about the importance of assessing cardiorespiratory fitness (CRF). In the review, CRF was found to be a stronger predictor for early mortality than already established risk factors such as smoking, diabetes, and obesity [91]. CRF is a measure of many physiologic factors such as how well your lungs transports the oxygen from the air to the blood and how well your muscles can utilize the oxygen. AHA recommends that:

"At a minimum, all adults should have CRF estimated each year using a nonexercise algorithm during their annual healthcare examination. Clinicians may consider the use of submaximal exercise tests or field tests as alternatives, because these involve individual-specific exercise responses" - cite from [91].

One way of assessing CRF is by measuring or estimating maximal oxygen consumption, VO$_2$max [92, 93]. Measuring VO$_2$max directly requires expensive equipment and that the subject is capable of performing a cycle ergometer or treadmill test until exhaustion. An alternative method is to use non-exercise models [94–97]. These models are based on demographic data and often give a good rough estimation of VO$_2$max. However, when used on subjects or patients that are outside of the group of subjects that the models are based on, they are often incorrect [98, 99]. The performance of these models can be enhanced using resting intrinsic cardiac performance measures.

SCG has previously been investigated in relation to exercise capacity and Libonati and co-works showed that the Tei Index, derived from resting SCG was correlated to CRF [29, 50, 52]. Based on how long the subjects were able to run on a treadmill following the Bruce protocol, they were grouped into three groups. Libonati correlated the Tei Index to the groups and found that Tei Index was lowest in the group with the highest functional capacity [50]. In this study, VO$_2$max was not measured. To the best of my knowledge, investigation

of VO$_2$max and SCG has only been investigated before by Shandhi and Co-workers [59] and then further in a journal article published after our study and results, in 2020 [60]. This article does not investigate the signal morphology directly but builds a model based on the frequency content of features in the signal. Shandhi was not able to estimate VO$_2$max very well, but focused on the estimation of VO$_2$ during a walk test.

In this study, we explore how both timing intervals and amplitudes derived from the SCG correlates with VO$_2$max

Methods

Seventeen females and 9 males participated in the study. The female subjects participated in a 2 month training course at a local fitness center. The training consisted of high-intensity training in a combination of weight lifting and cardiorespiratory exercise. The training was one hour sessions, two times a week. The males did not participate in a training course. Thus, for the females two recording sessions were conducted, one before the two months training course and one after. For the men, only one recording session was carried out. The study was approved by the local scientific committee of Northern Jutland, Denmark (N-20160034) and participants signed written informed consent before participating in the study.

We recorded resting SCG, PCG, and ECG for 5 minutes with the subjects in a supine position. Accelerometer and electrodes were positioned as described in Section 4.1 in Fig 4.2. VO$_2$max was obtained with a maximal effort cycle ergometer test (Ergomedic Peak Bike 894, Monark, Vansbre, Sweden) and the Vyntus CXP gas analyzer. The protocol consisted of four minutes of warm-up with two minutes of 80W load followed by 2 minutes of 104W load. Following the warm-up period, the mask for the gas analysis was fitted around the nose and mouth of the subject and the VO$_2$max protocol was initiated. The load of the cycle ergometer was increased every minute and the subject was verbally encouraged to keep the cadence and keep going to exhaustion, at which the trial ended.

Average SCG beats for each subject was computed following the approach described in section 4.2. Fiducial points in the SCG were manually annotated using the framework from Study I [53]. Six fiducial points were used in the data analysis, see Fig 5.7.

From the SCG we derived a series of cardiac timing intervals between a selection of the fiducial points: IVCT (E_s to AO_{max}), LVET (AO_{max} to B_d) and mechanical systolic time (E_s to B_d). Further we derived the following peak-to-peak amplitudes AO_{pp}, from AO_{min} to AO_{max} and AC_{pp}, from AC_{min} to AC_{max}. Demographic as well as the SCG features were correlated to
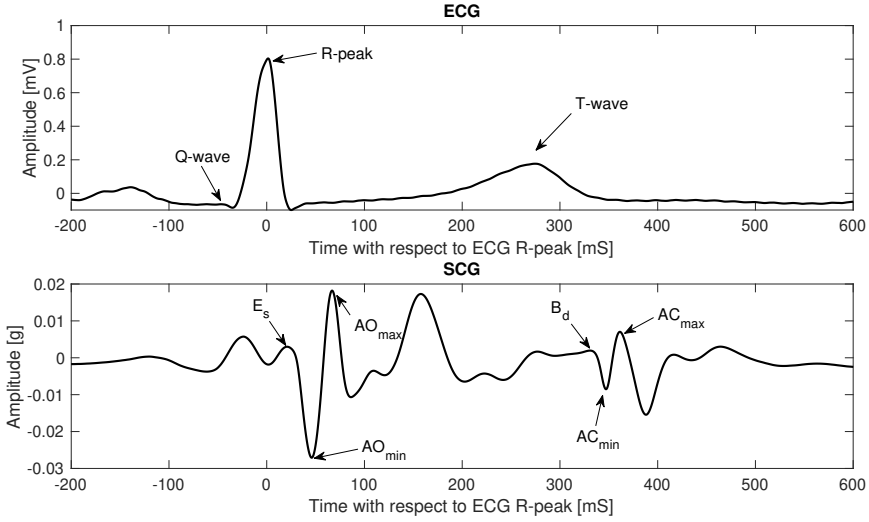
Fig. 5.7: Fiducial points used in the study. The E_s and AO_{max} location is correlated with the mitral valve close and aortic valve opening, respectively. B_d is correlated to the aortic valve closure. The three remaining locations are used for peak-to-peak amplitude calculation. ©Thieme Publishing Group. Reprint with permission from [78].

VO_2max. Using the MATLAB stepwise regression function, with demographic and seismocardiographic features as inputs, a linear regression model for VO_2max prediction was constructed. The model included age, sex, BMI and the amplitude AC_{pp}, see Equation 5.2. Correlation and standard error of the estimate (SEE) between the estimated and true VO_2max were computed. To investigate if the model was overfitted to the data, we computed both k-fold cross-validation (20 iterations with 10-fold validation) and Leave One Out (LOO) cross-validation. The performance of the model was compared to four other non-exercise models from peer-reviewed articles [94–97]. A model constructed only with the demographic data from the subjects participating in this study was also developed, see Equation 5.1. For both Equation 5.1 and 5.2, age is inputted as years and sex as 1 for male and 0 for females, and BMI as kg/m^2 and AC_{pp} is in milli-g.

$$VO_2\text{max} = 62.1 - .749 \cdot BMI + 9.94 \cdot SEX - .332 \cdot AGE \tag{5.1}$$

$$VO_2\text{max} = 44.1 - .465 \cdot BMI + 6.79 \cdot SEX - .187 \cdot AGE + .292 \cdot AC_{pp} \tag{5.2}$$

Results

The SCG feature used in the regression model (AC_{pp}) had a correlation to VO_2max of 0.80 (95% CI: 0.67-0.88, p < 0.001). Using this feature together

with demographic data in a linear prediction model for VO$_2$max, yielded a correlation of 0.90 (95% CI: 0.83-0.94) with a SEE of 3.18 mL·kg^{-1}·min^{-1}, see Figure 5.8. Both k-fold and LOO cross validation yielded a correlation of 0.87 between estimated and measured VO$_2$max. The demographic model (Equation 5.1) showed a correlation to VO$_2$max of 0.83 (95% CI: 0.72-0.90, p < 0.001) using all the data and 0.79 using LOO cross validation.

The model with the SCG feature (Equation 5.2) showed higher correlation and lower SEE than the four non-exercise prediction models that it was compared to when the models were used to predict VO$_2$max for the subjects in our study.
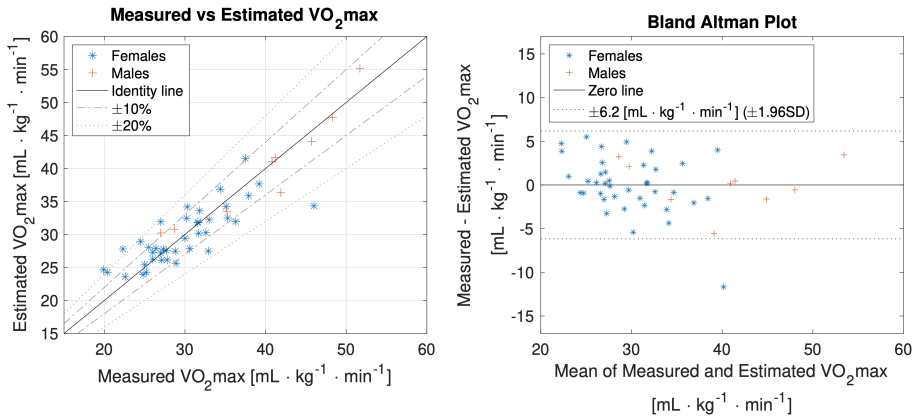
Fig. 5.8: Measured and predicted VO$_2$max using the model developed in the study. Correlation plot to the left and Bland Altman plot to the right. The model uses both demographic data and one feature from the SCG. ©Thieme Publishing Group. Reprint with permission from [78].

Conclusion

In this study, we show that there is a correlation between the SCG and VO$_2$max. We proposed the use of one of the easily recognizable features in the SCG in a non-exercise linear regression model for the prediction of VO$_2$max, a novel approach. A model with this feature could potentially be used in the clinic for estimation of CFR in subjects or patients that are not able to perform an ergometer test or in clinics that do not have the equipment needed to perform a maximal-effort test.

Chapter 5. Summary of Thesis Studies

Thesis Papers

The following three papers are based on the studies presented in this thesis.

6.1   Paper I

Definition of Fiducial Points in the Normal Seismocardiogram

Kasper Sørensen, Samuel E. Schmidt, Ask S. Jensen, Peter Søgaard and Johannes J. Struijk

6.2 Paper II

Seismocardiography as a Tool for Assessment of Bi-Ventricular Pacing

Kasper Sørensen, Peter Søgaard, Kasper Emerek, Ask S. Jensen, Johannes J. Struijk, Samuel E. Schmidt

In Review: Frontiers in Physiology - Cardiac Vibration Signals: Old Techniques, New Tricks and Applications (2020) November.

6.3 Paper III

A Clinical Method for Estimation of VO$_2$max using Seismocardiography

Kasper Sørensen, Mathias K. Poulsen, Dan S. Karbing, Peter Søgaard, Johannes J. Struijk and Samuel E. Schmidt

International Journal of Sports Medicine

Thieme

Chapter 6. Thesis Papers

Discussion

The following chapter will discuss the key findings from the three studies conducted in this Ph.D. thesis.

7.1 Main Findings

Three studies were conducted to fulfill the overall aim of the Ph.D.: to gain a better understanding of the seismocardiogram and find clinical applications for the method.

In Study I, SCG signals was obtained together with echocardiographic images from 45 healthy subjects. Based on this dataset eight fiducial points were defined in the SCG signals that correlated with eight physiologic events found in the echocardiographic images. Based on the data an overall mean SCG signal was created and used as the reference for the two other studies. In Study II, SCG signals from heart failure patients with implanted bi-ventricular pacemaker were analyzed. Turning on the pacemaker changed the cardiac timing intervals as well as the amplitudes derived from the SCG. This indicates that the SCG could potentially be used in a clinical application for CRT optimization. In study III, a prediction model for non-exercise VO_2max estimation was developed. The model uses simple demographic parameters (age, sex, and BMI) in combination with an amplitude feature derived from the SCG signal, and demonstrates for a potential clinical application of use for VO_2max estimation.

7.2 Fiducial Points of the Normal Seismocardiogram

One of the current disadvantages of SCG is that there is a lack of coherence in the nomenclature and interpretation of the signal between research articles [36, 43]. The first aim of this thesis was to gain a better understanding of the

SCG signal especially with respect to how the fiducial points in the signal correlate to physiologic events in the cardiac cycle. Since Patrick Mounsey described the SCG signal in 1956 there has been a shift from identifying the slopes of the signal to only look at the fiducial points. This makes sense as the fiducial points are relatively easily recognizable and consistent within the same subject over time [18]. However, it might also oversimplify the signal, to not study the slopes of the signal, as Mounsey did back in 1956.

In study I, we took a step back from the nomenclature that is used in the literature today and investigate all possible correlations between the fiducial points and physiologic events in the cardiac cycle. The method allowed for a combination of all the physiologic events found in the ultrasound images to be correlated and compared in time to the fiducial points from the SCG signals. Most of the fiducial point's locations in this study are the same as those of most other scientific articles published (for instance: [26, 28, 43, 100]). It does however introduce a location for the mitral valve opening, that is not commonly used, see Figure 5.5. The location we found for mitral valve opening does however correspond to the location used by Akhbardeh and co-workers, who also presents that the event could happen on the upwards stroke late in the diastolic phase [101]. The results from Akhbardeh are based on calculated acceleration from a simulation of a canine heart contraction, not an SCG recording from human subjects.

In the same time of publishing our result, Taebi and co-workers published the review *"Recent Advances in Seismocardiography"*, describing use cases, strengths, and limitations to the SCG signal [36]. This review also highlights the lack of accepted standards with respect to the definition of the fiducial points.

Using the fiducial points, the SCG signals from the healthy subjects were divided into sections, resampled to a mean length and reassembled again to provide an overall mean SCG signal, based on multiple subjects, see Figure 5.5. This overall mean SCG was used as a reference for the rest of the studies in the thesis when annotating fiducial points. Figure 5.5 also visualizes the 95% CI for the physiologic events found in the echocardiographic images for each of the eight fiducial points. This indicates, that the event found in the echo does not always coincide with the fiducial point, but that the event might as well be found along the slope leading towards the fiducial point, as Mounsey described it.

The reference for physiologic events used in Study I is echocardiographic images. For the recording of the cardiac contraction in near real-time, this method was the only available option. The method is however not without drawbacks. The temporal resolution is low compared to that of the SCG. Thus, rapid deflections in the SCG signal are not obtainable in the echo images. When annotating the ultrasound images it can be difficult to objectively mark for instance the beginning and end of an event - the operator has to make a

qualified decision as to where he/she thinks the colors and/or waveform has shifted enough to call it the start of an event. An alternative to this method could be to implement an algorithm for detection of the physiologic events like the algorithm described by Sørensen et al [102] or implement a homogeneous approach for describing the cardiac cycle, as described by Piras et al [103]. The latter might also be of value for describing the slopes of the signal, not only the fiducial points.

In the study, the R-peak of the ECG was used as a common reference for the SCG and echocardiographic images, as this was easily recognized in the echo images. Another approach could have been to use the onset of the Q-wave, indicating the start of the electrical activation and the mechanical contraction [6]. The Q-onset was used as a reference in the work by Dehkordi and co-workers [12]. For our study we found, that the Q-wave was more difficult to precisely annotate compared to the R-peak.

7.3 Using Seismocardiography to Assess Bi-Ventricular Pacemaker

In Study II, the number of patients was limited. 14 subjects had the complete dataset needed to be part of the data analysis. This naturally impacted the results and it is difficult to analyze for trends in the data with these few samples. Further, the SCG recordings from the CRT patients was in some cases difficult to interpret. The dyssynchronous nature of the cardiac contraction for these patients is very different from the normal healthy subjects which are reflected in the SCG signals. This makes it more difficult to annotate the signals but it also highlights that these patients require treatment.

For all but three patients, IVCT derived from SCG was improved as a response to turning on the pacemaker. This highlights the importance of the treatment as shorter IVCT is generally associated with improved cardiac contractility [46]. It might, however, also demonstrate that perhaps not all patients benefit from the treatment [104], at least when analyzing only the SCG signals. For the echo-images, the clinician assessed that IVCT improved for all the patients.

Novel to the study performed by Marcus and co-workers in 2007, we also investigated the amplitude of the SCG signal. One amplitude in the systolic complex was significantly higher when turning on the pacemaker as well as the amplitude between the minimum and maximum in the systolic complex. The first amplitude correlates well with the shortening in IVCT, calculated based on fiducial points in the same part of the complex. The shorter IVCT would cause a faster pressure buildup in the ventricle, thus also causing a

faster acceleration in the SCG signal. This underlines the mechanical changes to the CRT: pacing with the pacemaker affects the systolic complex of the cardiac cycle.

IVCT and IVRT derived from the SCG in our study were shorter than those reported by Marcus [46]. This could be due to the difference in the used fiducial points.

Another important finding in this study is, that dependent on the pacemaker setting, different fiducial points result in the highest correlation and lowest temporal difference between SCG and echo. When the bi-ventricular pacemaker was turned on, using G_s as an indicator for AO resulted in the highest correlation between SCG and echo for IVCT and LVET. However, the temporal difference was lower for both time intervals, using J_s as an indicator for AO. With the pacemaker turned off, the correlation between SCG and echo for IVCT was higher using J_s as an indicator for AO. Likewise, the temporal difference was also lower, using J_s compared to G_s. This raises the question, whether or not using G_s as a fiducial point for locating the AO is accurate in all subjects/patients. For the healthy subjects, the temporal difference between SCG and echo is the lowest, using G_s, but this is not the case for the CRT patients.

Another interesting observation is, that turning on the pacemaker makes the morphology of the SCG beats look a lot more like the "normal SCG" we created from the data in Study I. This is, of course, a subjective measure, but the implementation of something like the graph similarity score implemented by Inan and co-worker might be able to differentiate between SCG signals recorded with the pacemaker turned on and off [35]. With the experience of having seen multiple different SCG signals, one will become familiar with the "normal SCG". Thus, determining if an SCG is normal or not, might be an easy task for a trained clinician.

It has previously been observed, that some patients with prolonged QRS had no mechanical dyssynchrony and vice versa, patients with narrow QRS had mechanical dyssynchrony [14, 105–107]. Thus, to establish whether or not these patients have mechanical dyssynchrony another modality than ECG is necessary. Currently, this modality is echocardiography, but in the future SCG could be a good modality for this assessment. This would require a larger study population to investigate more configurations of the SCG signal.

SCG might be used as a tool in private practitioners clinics to screen for mechanical dyssynchrony, before referring the patients to the hospital to see a cardiologist.

7.4 Improving Non-Exercise Cardiorespiratory Fitness Estimation with Seismocardiography

In contrast to other non-exercise models for estimation of VO_2max, the model developed in Study III includes a feature derived from the SCG that by itself had a high correlation to VO_2max.

A drawback to the approach used is, that the feature was selected based on the whole dataset, which can induce bias into the feature selection. One way to solve this potential issue could be to divide the data set into three: a training set, a test set, and a validation set. The model and feature selection could then be performed based on the training set, tested on the test set, and finally validated on the validation set. Keeping the validation data set hidden when training the model, only using the test set to optimize the parameters could potentially make the model more generalizable. To check for overfitting, cross-validation was implemented, for K-fold cross-validation and leave one subject out cross-validation. Both showed good results with the implemented model, as reported in Section 5.3.

According to the Frank-Starling law, faster relaxation and increased diastolic filling would contribute to an increase in cardiac output and stroke volume, and thus improvement in VO_2max, highlighting the importance of the improvement in the diastolic complex [29, 108–112]. This can be described using the Fick equation, see Equation 7.1.

$$VO_2 = CO \cdot (C_a - C_v) \tag{7.1}$$

Where CO is the cardiac output, C_a is the oxygen concentration on the arterial blood and C_v is the oxygen concentration in the venous blood. Studies by Sutten et al. and Hagberg et al. reports that peak difference in arterial and venous oxygen concentration is not much different when comparing non-athletes to elite athletes [113, 114]. Thus, the major factor of a higher VO_2max is caused by a larger CO [112]. The Fick equation can be re-written, in terms of stroke volume (SV) and heart rate (HR), and further using end diastolic volume (EDV) and end systolic volume (ESV), see Equation 7.2.

$$\begin{aligned} VO_2 &= SV \cdot HR \cdot (C_a - C_v) \\ &= (EDV - ESV) \cdot HR \cdot (C_a - C_v) \end{aligned} \tag{7.2}$$

As the maximum heart rate for athletes have not been reported higher compared to non-athletes and because ESV is slightly increased in athletes compared to non-athletes, this leaves EDV as the most important factor contributing to a larger VO_2 [112]. Larger EDV can be achieved by enhanced cardiac

chamber compliance. To fill the larger volume with blood at high HR, rapid diastolic relaxation and suction must occur [112, 115].

The feature selected by the step-wise linear regression method is associated with the aortic valve closure [53, 78]. Gledhill and co-workers and Matsuda and co-workers showed that for athletes, ventricular relaxation is faster compared to normal subjects, which could explain why the amplitude has a high correlation to VO$_2$max, [109, 116]. Faster relaxation would result in a faster drop in pressure in the left ventricle, and thus a greater difference between the left ventricular and ascending aortic pressure. This could result in a larger amplitude in the area around the aortic valve closure derived from the SCG.

The model developed did not perform well in the estimation of changes in the VO$_2$max. Delta estimated VO$_2$max had a non-significant correlation to actual delta VO$_2$max of only 0.22 [78]. The low correlation could be due to the relatively short training period of two months, in which the heart muscle might not have been able to adapt. The higher VO$_2$max that is observed post-training for most of the subjects could thus also be attributed to an increase in blood volume, a response that has previously been documented to happen within as little as eight days of consecutive training [117], again due to the increased filling. Further, the overall change in VO$_2$max is quite small: 2.6 mL·kg^{-1}·min^{-1}. The day-to-day variability of the measured reference VO$_2$max measured with the Vyntus CPX has been reported to be 1.8 ± 2.2 %, which is approximately 70 % of the observed change for our study [118]. A longer follow-up period for subjects that would keep exercising regularly could be of interest, to investigate the potential long term changes to the cardiac muscle.

An aspect to investigate in future studies is the repeatability of estimation of VO$_2$max with this method. For subjects/patients at risk of early death, it may be more interesting to follow the trend and development in VO$_2$max as a result of increased exercise and change in everyday life habits, than it is to know the exact VO$_2$max. According to Ross et al., even a small and for most persons achievable improvement of 1 metabolic equivalent (MET) (about 3.5 mL·kg^{-1}·min^{-1}) in CRF is associated with an improvement in survival of 10-25 % [91]. Thus, being able to accurately track these small changes is desirable for a clinical application.

In mid-2020 Shandhi and co-workers published the full article of an initial conference abstract, demonstrating their approach for estimation of VO$_2$ during a treadmill test on both healthy and heart failure patients [59, 60]. The approach was slightly different compared to the one applied in Study III, as Shandhi estimated the VO$_2$ with an SCG signal recorded in the upper part of the sternum, while the subjects were in motion. Also, the study did not focus

as much on VO_2max and the model they developed did not perform well for VO_2max estimation (correlation between estimated and actual VO_2max: 0.5) [60].

7.5 Methodological Considerations

For all the studies performed as part of this thesis, mean beats have been used when deriving cardiac timing intervals and amplitudes from the SCG. This approach was applied to ensure that the beat was representative for the whole SCG recording, in some cases consisted of two to three minutes of recording. The approach ensures that the beat is less polluted with noise, without the use of much filtering. Changes to the signal due to for instance respiration, involuntary muscle contractions and peristaltic sounds are also mitigated. One downside to this approach is that potentially valuable beat-to-beat variations are also lost. For future studies, examinations of the individual cycle could bring information about cardiac contraction and relaxation. For instance, Dehkordi applied a method for recording echocardiogram, ECG, and SCG simultaneously being able to identify the same individual beats in all the modalities [12]. This approach is a good alternative to the method applied for Study I, where SCG and echo were not recorded simultaneously but consecutively.

Study II and, especially, III are explorative, investigating a number of features in the SCG signal for potential clinical application. The number of subjects in these studies, and especially study II, is limited and these studies require further research to validate whether or not the observed clinical benefits also apply to the general population.

In Study II we found that the correlation to the fiducial point associated with AO changed based on pacemaker setting. This is naturally of concern, and highlights the still present limitations of using the fiducial points in the SCG.

7.6 Scientific Contribution

The studies presented in this Ph.D. thesis contributes to both the fundamental understanding of the SCG signal, with Study I describing the fiducial points in the normal SCG and studies II and III concerning two clinical applications.

Study I contributes with knowledge about the manifestation of the SCG signal, contributing to previous work from Mounsey, Zanetti, Crow and most recently Dehkordi [12, 19, 27, 28]. Alongside the article from Dehkordi in 2019

(that includes a long list of co-authors within the SCG field) Study I is one of the newer studies that thoroughly describes the origin of the SCG signal. Based on papers like these, one common robust framework for annotation of the SCG signals could facilitate the use of the method, possibly even with automatic segmentation and annotation [72, 119, 120]. Study I separates itself from other studies by including all the fiducial points in the SCG signal and correlating them to the events in the echocardiographic images, regardless of previous literature. The study presents a transparent framework for annotation of the fiducial points that can be used by other researchers.

Study II elaborated on the work of Frank Marcus from 2007 by also investigating the amplitudes of different features of the SCG signal in CRT patients [46]. We found that the amplitudes in the SCG signals for the CRT patients were generally significantly smaller compared to healthy subjects. IVCT was, as also demonstrated by Marcus, significantly longer for the CRT patients when the pacemaker was turned off compared to a group of healthy subjects. Turning on the pacemaker shortened the IVCT to be no different than the healthy subjects. The study adds knowledge and insight into heart failure SCG signals and demonstrates a possible clinical application for SCG.

Study III demonstrates the correlation between the amplitudes of the SCG and cardiorespiratory fitness. This has, to the best of my knowledge, not been done yet. Shandhi and co-workers did examine how SCG could be used in the estimation of VO_2 and VO_2max, but the approach for analyzing the SCG signal was based on features of the signal, not the simple amplitude measure that we present [60]. The amplitudes of the SCG are not commonly investigated and research papers are often more concerned about the timing intervals derived from the SCG. Only a few studies have been examining the amplitudes and morphology of the signal, for instance, Salerno and Wilson proposed criteria for detecting CAD using exercise SCG based on the morphology of the signal [32, 33]. Inan and co-works investigated how the graph-similarity score can be used to assess the clinical status of heart failure patients [35]. The semi-novel approach of using the amplitudes of the SCG signal can hopefully be adopted by other researchers.

7.7 Future Perspectives for Seismocardiography

The use of SCG as an easy, in-expensive and non-invasive method for estimation of cardiac timing intervals and even overall assessment of cardiac healthy seems promising. The number of published articles is currently increasing and more researchers are taking advantage of the relatively cheap equipment that is available.

Even though the technique is not new the very fundamental research is still lagging, compared to technologies such as ECG or echocardiography. As much as we do understand about the signal, there is still a lot we do not understand. The origins of the most common fiducial points are well documented, but the slope or fiducial point related to the mitral valve opening is not concurrent among researchers - making it difficult to derive cardiac timing intervals that involve this physiologic event.

With a consensus about how to label the fiducial points or the slopes of the SCG signal, comparing results across research articles would most likely be easier allowing for further research into the different use cases of SCG. Having a common way of interpreting the signal is also, in my opinion, the only way to eventually convince clinical staff to implement the use of SCG in the clinic. Even though the signal is very deterministic it is also very complex and, as stated previously, not all the deflections in the signal are yet related to their underlying physiology.

Conclusion

In conclusion, this thesis presents a study that investigates the underlying physiologic origin of the signal with echocardiographic images as the reference to gain a better understanding of the signals physiologic origin. Using this knowledge, two studies demonstrate potential clinical use cases for the SCG. Study II documents how the SCG manifests in patients with LBBB and how the SCG can be used to assess the bi-ventricular pacemaker treatment. Study III investigates and documents how the signal correlates to VO_2max and demonstrates a novel use for SCG in the non-exercise estimation of cardiorespiratory fitness.

References

[1] Elizabeth Wilkins et al. "European Cardiovascular Disease Statistics 2017". In: *European Heart Network* (Feb. 2017).

[2] Sameer Bansilal, José M Castellano, and Valentín Fuster. "Global Burden of CVD: Focus on Secondary Prevention of Cardiovascular Disease". In: *International journal of cardiology* 201 (2015), S1–S7. DOI: 10.1016/s0167-5273(15)31026-3.

[3] European Heart Network. *Heart Failure and Cardiovascular Diseases – A European Heart Network Paper*. Apr. 2019.

[4] Virani Salim S. et al. "Heart Disease and Stroke Statistics—2020 Update: A Report From the American Heart Association". In: *Circulation* 141.9 (Mar. 2020), e139–e596. DOI: 10.1161/cir.0000000000000757.

[5] Frederic H Martini and Judi L Nath. *Fundamentals of Anatomy and Physiology*. Eighth. Pearson. ISBN: 0-321-53910-9.

[6] Valentin Fuster et al. *Hurst's The Heart*. 11 edition. McGraw-Hill Professional, May 2004. ISBN: 0-07-142264-1.

[7] Howard B. Sprague. "History and Present Status of Phonocardiography". In: *IRE Transactions on Medical Electronics* PGME-9 (Dec. 1957), pp. 2–3. DOI: 10.1109/iret-me.1957.5008615.

[8] R. C. Schlant et al. "Guidelines for Electrocardiography. A Report of the American College of Cardiology/American Heart Association Task Force on Assessment of Diagnostic and Therapeutic Cardiovascular Procedures (Committee on Electrocardiography)." In: *Circulation* 85 (1992), pp. 1221–1228. DOI: 10.1161/01.cir.85.3.1221.

[9] Willem Einthoven. "Die Galvanometrische Registrirung Des Menschlichen Elektrokardiogramms, Zugleich Eine Beurtheilung Der Anwendung Des Capillar-Elektrometers in Der Physiologie". In: *Archiv für die gesamte Physiologie des Menschen und der Tiere* 99.9-10 (1903), pp. 472–480. DOI: 10.1007/bf01811855.

[10] I Edler and CH Hertz. "Use of Ultrasonic Reflectoscope for Continuous Recording of Movements of Heart Walls". In: *Kungl. Fysiografiska Sållskapets I Lund Förhandlingar* 24.5 (1954).

[11]   Catherine M. Otto MD. *Textbook of Clinical Echocardiography: Expert Consult - Online and Print*. 4 edition. Philadelphia, PA: Saunders, July 2009. ISBN: 978-1-4160-5559-4.

[12]   Parastoo Dehkordi et al. "Comparison of Different Methods for Estimating Cardiac Timings: A Comprehensive Multimodal Echocardiography Investigation". In: *Frontiers in Physiology* 10 (2019), p. 1057. DOI: 10.3389/fphys.2019.01057.

[13]   Mary Ann Peberdy and Joseph P. Ornato. "Recognition of Electrocardiographic Lead Misplacements". In: *The American Journal of Emergency Medicine* 11.4 (July 1993), pp. 403–405. DOI: 10.1016/0735-6757(93)90177-D.

[14]   David A Kass. "Cardiac Resynchronization Therapy". In: *Journal of Cardiovascular Electrophysiology* 16.s1 (2005), S35–S41. DOI: 10.1111/j.1540-8167.2005.50136.x.

[15]   Josep Brugada et al. "Contractility Sensor-Guided Optimization of Cardiac Resynchronization Therapy: Results from the RESPOND-CRT Trial". In: *European Heart Journal* 38.10 (2016), pp. 730–738. DOI: 10.1093/eurheartj/ehw526.

[16]   John Gorcsan III et al. "Echocardiography for Cardiac Resynchronization Therapy: Recommendations for Performance and Reporting–a Report from the American Society of Echocardiography Dyssynchrony Writing Group Endorsed by the Heart Rhythm Society". In: *Journal of the American Society of Echocardiography* 21.3 (2008), pp. 191–213. DOI: 10.1016/j.echo.2008.01.003.

[17]   Martin Vandborg Andersen. "Contraction Fronts of the Left Cardiac Ventricle". PhD thesis. Aalborg University, 2019.

[18]   John M. Zanetti and David M. Salerno. "Seismocardiography: A New Technique for Recording Cardiac Vibrations. Concept, Method, and Initial Observations". In: *Journal of Cardiovascular Technology* 9.2 (1990), pp. 111–118.

[19]   Patrick Mounsey. "Praecordial Ballistocardiography". In: *British Heart Journal* 19.2 (1957), pp. 259–271. DOI: 10.1136/hrt.19.2.259.

[20]   M. Di Rienzo et al. "Wearable Seismocardiography: Towards a Beat-by-Beat Assessment of Cardiac Mechanics in Ambulant Subjects". In: *Autonomic Neuroscience: Basic and Clinical* 178.1-2 (2013), pp. 50–59. DOI: 10.1016/j.autneu.2013.04.005.

[21]   John M Zanetti and Kouhyar Tavakolian. "Seismocardiography: Past, Present and Future". In: *35th Annual International Conference of the IEEE Engineering in Medicine and Biology Society (EMBC)* (2013), pp. 7004–7007. DOI: 10.1109/embc.2013.6611170.

[22] Robert V Elliott, Robert G A Y Packard, and Demos T Kyrazis. "Acceleration Ballistocardiography: Design, Construction, and Application of a New Instrument". In: *Circulation* 9.2 (1954), pp. 281–291. DOI: 10.1161/01.cir.9.2.281.

[23] Yandell Henderson. "The Mass-Movements of the Circulation as Shown by a Recoil Curve". In: *American Journal of Physiology* 14.3 (1905), pp. 287–298. DOI: 10.1152/ajplegacy.1905.14.3.287.

[24] B S Bozhenko. "Seismocardiography-a New Method in the Study of Functional Conditions of the Heart". In: *Terapevticheskii arkhiv* 33 (1961), pp. 55–64.

[25] R M Baevskii. *Physiological Methods in Astronautics*. Tech. rep. Air Force Syst. Comand, Foreign Technology Division, 1966.

[26] John M. Zanetti and David M Salerno. "Seismocardiography: A Technique for Recording Precordial Acceleration". In: Computer-Based Medical Systems, 1991. Proceedings of the Fourth Annual IEEE Symposium. IEEE, 1991, pp. 4–9. DOI: 10.1109/cbms.1991.128936.

[27] John M. Zanetti, M O Poliac, and Richard S Crow. "Seismocardiography: Waveform Identification and Noise Analysis". In: Computers in Cardiology. IEEE, 1991, pp. 49–52. DOI: 10.1109/cic.1991.169042.

[28] Richard S Crow et al. "Relationship between Seismocardiogram and Echocardiogram for Events in the Cardiac Cycle". In: *American Journal of Noninvasive Cardiology* 8.1 (1994), pp. 39–46. DOI: 10.1159/000470156.

[29] Joseph R Libonati et al. "Systolic and Diastolic Cardiac Function Time Intervals and Exercise Capacity in Women." In: *Medicine and Science in Sports and Exercise* 31.2 (Feb. 1999), pp. 258–263. DOI: 10.1097/00005768-199902000-00009.

[30] David M. Salerno et al. "Seismocardiographic Changes Associated with Obstruction of Coronary Blood Flow during Balloon Angioplasty". In: *The American Journal of Cardiology* 68.2 (July 1991), pp. 201–207. DOI: 10.1016/0002-9149(91)90744-6.

[31] David M Salerno and John Zanetti. "Seismocardiography for Monitoring Changes in Left Ventricular Function during Ischemia." In: *CHEST Journal* 100.4 (1991), pp. 991–993. DOI: 10.1378/chest.100.4.991.

[32] David M Salerno et al. "Exercise Seismocardiography for Detection of Coronary Artery Disease". In: *American Journal of Noninvasive Cardiology* 6 (1992), pp. 321–330. DOI: 10.1159/000470383.

[33] Richard A. Wilson et al. "Diagnostic Accuracy of Seismocardiography Compared with Electrocardiography for the Anatomic and Physiologic Diagnosis of Coronary Artery Disease during Exercise Testing". In: *The American Journal of Cardiology* 71.7 (1993), pp. 536–545. DOI: 10.1016/0002-9149(93)90508-a.

[34] Parastoo Dehkordi et al. "Identifying Patients with Coronary Artery Disease Using Rest and Exercise Seismocardiography". In: *Frontiers in Physiology* 10 (2019). DOI: 10.3389/fphys.2019.01211.

[35] Omer T Inan et al. "Novel Wearable Seismocardiography and Machine Learning Algorithms Can Assess Clinical Status of Heart Failure Patients". In: *Circulation: Heart Failure* 11.1 (2018), e004313. DOI: 10.1161/circheartfailure.117.004313.

[36] Amirtahà Taebi et al. "Recent Advances in Seismocardiography". In: *Vibration* 2.1 (Jan. 2019), pp. 64–86. DOI: 10.3390/vibration2010005.

[37] Kouhyar Tavakolian et al. "Estimation of Hemodynamic Parameters from Seismocardiogram". In: *Computing in Cardiology*. Sept. 2010, pp. 1055–1058.

[38] Kouhyar Tavakolian et al. "Precordial Acceleration Signals Improve the Performance of Diastolic Timed Vibrations". In: *Medical Engineering & Physics* 35.8 (2013), pp. 1133–1140. DOI: 10.1016/j.medengphy.2012.12.001.

[39] Chenxi Yang and Negar Tavassolian. "Pulse Transit Time Measurement Using Seismocardiogram, Photoplethysmogram, and Acoustic Recordings: Evaluation and Comparison". In: *IEEE Journal of Biomedical and Health Informatics* 22.3 (2018), pp. 733–740. DOI: 10.1109/jbhi.2017.2696703.

[40] Ajay K Verma et al. "Pulse Transit Time Extraction from Seismocardiogram and Its Relationship with Pulse Pressure". In: *Computing in Cardiology Conference (CinC)*. IEEE, 2015, pp. 37–40.

[41] Marco Di Rienzo, Emanuele Vaini, and Prospero Lombardi. "Use of Seismocardiogram for the Beat-to-Beat Assessment of the Pulse Transit Time: A Pilot Study". In: *Engineering in Medicine and Biology Society (EMBC), 2015 37th Annual International Conference of the IEEE*. IEEE, 2015, pp. 7184–7187. DOI: 10.1109/embc.2015.7320049.

[42] Kasper Sørensen et al. "Challenges in Using Seismocardiography for Blood Pressure Monitoring". In: *Computing in Cardiology* 44 (2017), p. 1.

[43] Omer Inan et al. "Ballistocardiography and Seismocardiography: A Review of Recent Advances". In: *IEEE Journal of Biomedical and Health Informatics* PP.99 (2015), pp. 1–1. DOI: 10.1109/jbhi.2014.2361732.

[44] Heiko Gesche et al. "Continuous Blood Pressure Measurement by Using the Pulse Transit Time: Comparison to a Cuff-Based Method". In: *European Journal of Applied Physiology* 112.1 (Jan. 2012), pp. 309–315. DOI: 10.1007/s00421-011-1983-3.

[45] Ramakrishna Mukkamala et al. "Toward Ubiquitous Blood Pressure Monitoring via Pulse Transit Time: Theory and Practice". In: *IEEE Transactions on Biomedical Engineering* 62.8 (2015), pp. 1879–1901. DOI: 10.1109/tbme.2015.2441951.

[46] Frank I Marcus et al. "Accelerometer-Derived Time Intervals during Various Pacing Modes in Patients with Biventricular Pacemakers: Comparison with Normals". In: *PACE - Pacing and Clinical Electrophysiology* 30.12 (2007), pp. 1476–1481. DOI: 10.1111/j.1540-8159.2007.00894.x.

[47] Lionel Giorgis et al. "Analysis of Cardiac Micro-Acceleration Signals for the Estimation of Systolic and Diastolic Time Intervals in Cardiac Resynchronization Therapy". In: *Computers in Cardiology*. IEEE, 2008, pp. 393–396.

[48] Lionel Giorgis et al. "Optimal Algorithm Switching for the Estimation of Systole Period from Cardiac Microacceleration Signals (Sonr)". In: *IEEE Transactions on Biomedical Engineering* 59.11 (2012), pp. 3009–3015. DOI: 10.1109/tbme.2012.2212019.

[49] E. Donal et al. "Endocardial Acceleration (sonR) vs. Ultrasound-Derived Time Intervals in Recipients of Cardiac Resynchronization Therapy Systems". In: *Europace* 13.3 (Mar. 2011), pp. 402–408. DOI: 10.1093/europace/euq411.

[50] J R Libonati, J Ciccolo, and H Glassber G. "The Tei Index and Exercise Capacity." In: *The Journal of Sports Medicine and Physical Fitness* 41.1 (Mar. 2001), pp. 108–113.

[51] Anh Dinh, Francis M Bui, and Tam Nguyen. "An Accelerometer Based System to Measure Myocardial Performance Index during Stress Testing". In: Engineering in Medicine and Biology Society (EMBC), 2016 IEEE 38th Annual International Conference of The. IEEE, 2016, pp. 4877–4880. DOI: 10.1109/embc.2016.7591820.

[52] C Tei, L H Ling, D O Hodge, et al. "New Index of Combined Systolic and Diastolic Myocardial Performance: A Study in Normals and Dilated Cardiomyopathy". In: *Journal of Cardiology* 26.6 (1995), pp. 357–366.

[53] Kasper Sørensen et al. "Definition of Fiducial Points in the Normal Seismocardiogram". In: *Scientific Reports* 8.1 (2018), p. 15455. DOI: 10.1038/s41598-018-33675-6.

[54] Marco Di Rienzo et al. "MagIC System: A New Textile-Based Wearable Device for Biological Signal Monitoring. Applicability in Daily Life and Clinical Setting". In: *IEEE Engineering in Medicine and Biology 27th Annual Conference*. IEEE, 2006, pp. 7167–7169.

[55] Paolo Castiglioni et al. "Wearable Seismocardiography". In: *29th Annual International Conference of the IEEE Engineering in Medicine and Biology Society*. IEEE, 2007, pp. 3954–3957. DOI: 10.1109/iembs.2007.4353199.

[56] Marco Di Rienzo et al. "A Wearable System for the Seismocardiogram Assessment in Daily Life Conditions". In: *Proceedings of the Annual International Conference of the IEEE Engineering in Medicine and Biology Society, EMBS* (2011), pp. 4263–4266. DOI: 10.1109/iembs.2011.6091058.

[57] Marco Di Rienzo, Emanuele Vaini, and Prospero Lombardi. "Development of a Smart Garment for the Assessment of Cardiac Mechanical Performance and Other Vital Signs during Sleep in Microgravity". In: *Sensors and Actuators A: Physical* 274 (2018), pp. 19–27. DOI: 10.1016/j.sna.2018.02.034.

[58] Marco Di Rienzo et al. "SeisMote: A Multi-Sensor Wireless Platform for Cardiovascular Monitoring in Laboratory, Daily Life, and Telemedicine". In: *Sensors* 20 (2020), pp. 680–. DOI: 10.3390/s20030680.

[59] Md. Mobashir Hasan Shandhi et al. "Seismocardiography Can Assess Cardiopulmonary Exercise Test Parameters in Patients with Heart Failure". In: *Journal of Cardiac Failure* 24.8, Supplement (2018), S124–S125. DOI: 10.1016/j.cardfail.2018.07.446.

[60] Md Mobashir Hasan Shandhi et al. "Wearable Patch-Based Estimation of Oxygen Uptake and Assessment of Clinical Status during Cardiopulmonary Exercise Testing in Patients with Heart Failure". In: *Journal of Cardiac Failure* (2020). DOI: 10.1016/j.cardfail.2020.05.014.

[61] Olli Lahdenoja et al. "A Smartphone-Only Solution for Detecting Indications of Acute Myocardial Infarction". In: *IEEE EMBS International Conference on Biomedical & Health Informatics (BHI),* (2017), pp. 197–200. DOI: 10.1109/bhi.2017.7897239.

[62] Saeed Mehrang et al. "Machine Learning Based Classification of Myocardial Infarction Conditions Using Smartphone-Derived Seismo- and Gyrocardiography". In: *Computing in Cardiology* 2018-September (2018). DOI: 10.22489/cinc.2018.110.

[63] Olli Lahdenoja et al. "Atrial Fibrillation Detection via Accelerometer and Gyroscope of a Smartphone". In: *IEEE journal of biomedical and health informatics* 22 (2018), pp. 108–118. DOI: 10.1109/jbhi.2017.2688473.

[64] Marco Di Rienzo, Emanuele Vaini, and Prospero Lombardi. "An Algorithm for the Beat-to-Beat Assessment of Cardiac Mechanics during Sleep on Earth and in Microgravity from the Seismocardiogram". In: *Scientific Reports* 7.1 (2017). DOI: 10.1038/s41598-017-15829-0.

[65] Johan Wahlström et al. "A Hidden Markov Model for Seismocardiography". In: *IEEE Transactions on Biomedical Engineering* 64.10 (2017), pp. 2361–2372. DOI: 10.1109/tbme.2017.2648741.

[66] Farzad Khosrow-Khavar et al. "Automatic Annotation of Seismocardiogram with High Frequency Precordial Accelerations." In: *IEEE journal of biomedical and health informatics* 2194.c (2014), pp. 1428–1434. DOI: 10.1109/jbhi.2014.2360156.

[67] Farzad Khosrow-Khavar et al. "Automatic and Robust Delineation of the Fiducial Points of the Seismocardiogram Signal for Noninvasive Estimation of Cardiac Time Intervals". In: *IEEE Transactions on Biomedical Engineering* 64.8 (2017), pp. 1701–1710. DOI: 10.1109/tbme.2016.2616382.

[68] Farzad Khosrow-Khavar, Kouhyar Tavakolian, and Carlo Menon. "Moving toward Automatic and Standalone Delineation of Seismocardiogram Signal." In: *Annual International Conference of the IEEE Engineering in Medicine and Biology Society.* 2015 (2015), pp. 7163–6. DOI: 10.1109/embc.2015.7320044.

[69] Prasan Kumar Sahoo et al. "On the Design of an Efficient Cardiac Health Monitoring System through Combined Analysis of ECG and SCG Signals". In: *Sensors* 18.2 (2018), p. 379. DOI: 10.3390/s18020379.

[70] Ghufran Shafiq, Sivanagaraja Tatinati, and Kalyana C. Veluvolu. "Automatic Annotation of Peaks in Seismocardiogram for Systolic Time Intervals". In: *38th Annual International Conference of the IEEE Engineering in Medicine and Biology Society (EMBC)* 2016 (Oct. 2016), pp. 2672–2675. DOI: 10.1109/embc.2016.7591280.

[71] Tilendra Choudhary, L N Sharma, and M K Bhuyan. "Automatic Detection of Aortic Valve Opening Using Seismocardiography in Healthy Individuals." In: *IEEE journal of biomedical and health informatics* 23.3 (2019), pp. 1032–1040. DOI: 10.1109/jbhi.2018.2829608.

[72] Niccolò Mora et al. "A Unified Methodology for Heartbeats Detection in Seismocardiogram and Ballistocardiogram Signals". In: *Computers* 9.2 (June 2020), p. 41. DOI: 10.3390/computers9020041.

[73] Niccolò Mora et al. "Fully Automated Annotation of Seismocardiogram for Noninvasive Vital Sign Measurements". In: *IEEE Transactions on Instrumentation and Measurement* 69.4 (Apr. 2020), pp. 1241–1250. DOI: 10.1109/TIM.2019.2908511.

[74] Tilendra Choudhary, M. K. Bhuyan, and L. N. Sharma. "A Novel Method for Aortic Valve Opening Phase Detection Using SCG Signal". In: 20 (2020), pp. 899–908. DOI: 10.1109/jsen.2019.2944235.

[75] Chenxi Yang and Negar Tavassolian. "Combined Seismo-and Gyro-Cardiography: A More Comprehensive Evaluation of Heart-Induced Chest Vibrations". In: *IEEE Journal of Biomedical and Health Informatics* 22.5 (2018), pp. 1466–1475. DOI: 10.1109/jbhi.2017.2764798.

[76] Silicon Designs Inc. *SD1521 Datasheet*. 2018.

[77] Colibrys. *SF1600S.A Datasheet*. 2020.

[78] Kasper Sørensen et al. "A Clinical Method for Estimation of VO2max Using Seismocardiography". In: *International Journal of Sports Medicine* 41.10 (2020), pp. 661–668. DOI: 10.1055/a-1144-3369.

[79] Ask S Jensen et al. "Effects of Cardiac Resynchronization Therapy on the First Heart Sound Energy". In: *Computing in Cardiology* 41 (2014), pp. 29–32.

[80] Kasper Sørensen et al. "Seismocardiographic Correlations to Age, Gender and BMI". In: *39th Annual International Conference of the IEEE Engineering in Medicine and Biology Society*. 2017, Paper ThAT5.4.

[81] Tor Biering-Sørensen et al. "Cardiac Time Intervals by Tissue Doppler Imaging M-Mode: Normal Values and Association with Established Echocardiographic and Invasive Measures of Systolic and Diastolic Function". In: *PLoS ONE* 11.4 (2016), pp. 1–14. DOI: 10.1371/journal.pone.0153636.

[82] Kasper Sørensen et al. "Changes of Seismocardiographic Intervals in Cardiac Resynchronization Therapy". In: *Computing in Cardiology*. Sept. 2019.

[83] Francisco Leyva, Seah Nisam, and Angelo Auricchio. "20 Years of Cardiac Resynchronization Therapy". In: *Journal of the American College of Cardiology* 64.10 (Sept. 2014), pp. 1047–1058. DOI: 10.1016/j.jacc.2014.06.1178.

[84] Samuele Baldasseroni et al. "Left Bundle-Branch Block Is Associated with Increased 1-Year Sudden and Total Mortality Rate in 5517 Outpatients with Congestive Heart Failure: A Report from the Italian Network on Congestive Heart Failure". In: *American heart journal* 143.3 (2002), pp. 398–405. DOI: 10.1067/mhj.2002.121264.

[85] Serge Cazeau et al. "Effects of Multisite Biventricular Pacing in Patients with Heart Failure and Intraventricular Conduction Delay". In: *New England Journal of Medicine* 344.12 (2001), pp. 873–880. DOI: `10.1056/nejm200103223441202`.

[86] S S Barold. "What Is Cardiac Resynchronization Therapy?" In: *American Journal of Medicine* 111.3 (2001), pp. 224–232. DOI: `10.1016/s0002-9343(01)00807-5`.

[87] Angelo Auricchio et al. "Long-Term Clinical Effect of Hemodynamically Optimized Cardiac Resynchronization Therapy in Patients with Heart Failure and Ventricular Conduction Delay". In: *Journal of the American College of Cardiology* 39.12 (2002), pp. 2026–2033. DOI: `10.1016/s0735-1097(02)01895-8`.

[88] Cecilia Linde, Kenneth Ellenbogen, and Finlay A. McAlister. "Cardiac Resynchronization Therapy (CRT): Clinical Trials, Guidelines, and Target Populations". In: *Heart Rythm* 9 (2012), S3–S13. DOI: `10.1016/j.hrthm.2012.04.026`.

[89] A. Zweerink et al. "Hemodynamic Optimization in Cardiac Resynchronization Therapy: Should We Aim for dP/Dtmax or Stroke Work?" In: *JACC: Clinical Electrophysiology* 5.9 (2019), pp. 1013–1025. DOI: `10.1016/j.jacep.2019.05.020`.

[90] Kasper Sørensen et al. "Correlation between Valve Event Amplitudes in the Seismocardiogram and VO2-Max". In: *Engineering in Medicine and Biology Conference*. 2019.

[91] Robert Ross et al. "Importance of Assessing Cardiorespiratory Fitness in Clinical Practice: A Case for Fitness as a Clinical Vital Sign: A Scientific Statement from the American Heart Association". In: *Circulation* 134.24 (2016), e653–e699. DOI: `10.1161/cir.0000000000000461`.

[92] A V Hill, C N H Long, and H Lupton. "Muscular Exercise, Lactic Acid, and the Supply and Utilisation of Oxygen". In: *Proceedings of the Royal Society B: Biological Sciences* 96.679 (Sept. 1924), pp. 438–475. DOI: `10.1098/rspb.1924.0037`.

[93] Massimo F Piepoli et al. "Statement on Cardiopulmonary Exercise Testing in Chronic Heart Failure Due to Left Ventricular Dysfunction: Recommendations for Performance and Interpretation. Part I: Definition of Cardiopulmonary Exercise Testing Parameters for Appropriate Use in Chroni". In: *European journal of cardiovascular prevention and rehabilitation: official journal of the European Society of Cardiology, Working Groups on Epidemiology & Prevention and Cardiac Rehabilitation and Exercise Physiology* 13.2 (2006), pp. 150–164. DOI: `10.1097/01.hjr.0000209812.05573.04`.

[94] Norman L Jones et al. "Normal Standards for an Incremental Progressive Cycle Ergometer Test". In: *American Review of Respiratory Disease* 131.5 (1985), pp. 700–708.

[95] Mary Sue Fairbarn et al. "Prediction of Heart Rate and Oxygen Uptake during Incremental and Maximal Exercise in Healthy Adults". In: *Chest* 105.5 (1994), pp. 1365–1369. DOI: 10.1378/chest.105.5.1365.

[96] Christopher B Cooper and Thomas W Storer. *Exercise Testing and Interpretation: A Practical Approach*. Cambridge University Press, 2001, pp. 220–221. DOI: 10.1378/chest.122.1.388-a.

[97] James A Davis et al. "Lower Reference Limit for Maximal Oxygen Uptake in Men and Women". In: *Clinical Physiology and Functional Imaging* 22.5 (2002), pp. 332–338. DOI: 10.1046/j.1475-097x.2002.00440.x.

[98] Fred W Kolkhorst and Forrest A Dolgener. "Nonexercise Model Fails to Predict Aerobic Capacity in College Students with High VO2peak". In: *Research Quarterly for Exercise and Sport* 65.1 (1994), pp. 78–83. DOI: 10.1080/02701367.1994.10762211.

[99] Moh H Malek et al. "A New Nonexercise-Based VO2max Equation for Aerobically Trained Females". In: *Medicine & Science in Sports & Exercise* 36.10 (2004), pp. 1804–1810. DOI: 10.1249/01.mss.0000142299.42797.83.

[100] Kouhyar Tavakolian. "Characterization and Analysis of Seismocardiogram for Estimation of Hemodynamic Parameters". PhD thesis. Applied Science: School of Engineering Science / Applied Science: School of Engineering Science, 2010.

[101] Alireza Akhbardeh et al. "Comparative Analysis of Three Different Modalities for Characterization of the Seismocardiogram". In: *Annual International Conference of the IEEE Engineering in Medicine and Biology Society*. IEEE, 2009, pp. 2899–2903. DOI: 10.1109/iembs.2009.5334444.

[102] Kasper Sørensen et al. "Automatic Segmentation of Mitral Leaflet Movement in Doppler Tissue M-Mode Ultrasound". In: *Computing in Cardiology*. Vol. 43. IEEE, 2016. DOI: 10.22489/cinc.2016.040-459.

[103] Paolo Piras et al. "Homeostatic Left Heart Integration and Disintegration Links Atrio-Ventricular Covariation's Dyshomeostasis in Hypertrophic Cardiomyopathy". In: *Scientific Reports* 7.1 (2017), pp. 1–12. DOI: 10.1038/s41598-017-06189-w.

[104] Angelo Auricchio and Frits W Prinzen. "Non-Responders to Cardiac Resynchronization Therapy". In: *Circulation Journal* 75 (2011), pp. 521–527. DOI: 10.1253/circj.cj-10-1268.

[105] Iris Schuster et al. "Diastolic Asynchrony Is More Frequent than Systolic Asynchrony in Dilated Cardiomyopathy and Is Less Improved by Cardiac Resynchronization Therapy". In: *Journal of the American College of Cardiology* 46 (2005), pp. 2250–2257. DOI: 10.1016/j.jacc.2005.02.096.

[106] CM Yu et al. "High Prevalence of Left Ventricular Systolic and Diastolic Asynchrony in Patients with Congestive Heart Failure and Normal QRS Duration". In: *Heart* 89.1 (2003), pp. 54–60. DOI: 10.1136/heart.89.1.54.

[107] Stefano Ghio et al. "Interventricular and Intraventricular Dyssynchrony Are Common in Heart Failure Patients, Regardless of QRS Duration". In: *European Heart Journal* 25.7 (2004), pp. 571–578. DOI: 10.1016/j.ehj.2003.09.030.

[108] Lars Juel Andersen et al. "Improvement of Systolic and Diastolic Heart Function after Physical Training in Sedentary Women". In: *Scandinavian Journal of Medicine & Science in Sports* 20 (2010), pp. 50–57. DOI: 10.1111/j.1600-0838.2009.01088.x.

[109] Norman Gledhill, Dean Cox, and Roni Jamnik. "Endurance Athletes' Stroke Volume Does Not Plateau: Major Advantage Is Diastolic Function." In: *Medicine and science in sports and exercise* 26.9 (1994), pp. 1116–1121. DOI: 10.1249/00005768-199409000-00008.

[110] Wayne C Levy et al. "Endurance Exercise Training Augments Diastolic Filling at Rest and during Exercise in Healthy Young and Older Men." In: *Circulation* 88.1 (1993), pp. 116–126. DOI: 10.1161/01.cir.88.1.116.

[111] C Gunnar Blomqvist and Bengt Saltin. "Cardiovascular Adaptations to Physical Training". In: *Annual Review of Physiology* 45.1 (1983), pp. 169–189. DOI: 10.1146/annurev.ph.45.030183.001125.

[112] Benjamin D Levine. "VO2-Max: What Do We Know, and What Do We Still Need to Know?" In: *The Journal of physiology* 586.1 (2008), pp. 25–34. DOI: 10.1113/jphysiol.2007.147629.

[113] J. M. Hagberg et al. "A Hemodynamic Comparison of Young and Older Endurance Athletes during Exercise". In: *Journal of Applied Physiology* 58.6 (June 1985), pp. 2041–2046. DOI: 10.1152/jappl.1985.58.6.2041.

[114] J. R. Sutton et al. "Operation Everest II: Oxygen Transport during Exercise at Extreme Simulated Altitude". In: *Journal of Applied Physiology* 64.4 (Apr. 1988), pp. 1309–1321. DOI: 10.1152/jappl.1988.64.4.1309.

[115] Edward L. Yellin, Srdjan Nikolic, and Robert W.M. Frater. "Left Ventricular Filling Dynamics and Diastolic Function". In: *Progress in Cardiovascular Diseases* 32.4 (Jan. 1990), pp. 247–271. DOI: 10.1016/0033-0620(90)90016-U.

[116] M Matsuda et al. "Effect of Exercise on Left Ventricular Diastolic Filling in Athletes and Nonathletes". In: *Journal of Applied Physiology* 55.2 (1983), pp. 323–328. DOI: 10.1152/jappl.1983.55.2.323.

[117] V A Convertino et al. "Exercise Training-Induced Hypervolemia: Role of Plasma Albumin, Renin, and Vasopressin". In: *Journal of Applied Physiology* 48.4 (1980), pp. 665–669. DOI: 10.1152/jappl.1980.48.4.665.

[118] Mathias Krogh Poulsen et al. "VO2, VCO2 and VE between-Day Reliability of the Vyntus CPX Metabolic Cart during Progressive Cycling". In: 2016.

[119] Hiren Kumar Thakkar and Prasan Kumar Sahoo. "Towards Automatic and Fast Annotation of Seismocardiogram Signals Using Machine Learning". In: *IEEE Sensors Journal* 20 (2020), pp. 2578–2589. DOI: 10.1109/jsen.2019.2951068.

[120] Federico Cocconcelli et al. "Seismocardiography-Based Detection of Heartbeats for Continuous Monitoring of Vital Signs". In: *11th Computer Science and Electronic Engineering (CEEC)* (2019), pp. 53–58. DOI: 10.1109/ceec47804.2019.8974343.